iScience

CellPress
OPEN ACCESS

Article

Rad52 SUMOylation functions as a molecular switch that determines a balance between the Rad51- and Rad59-dependent survivors

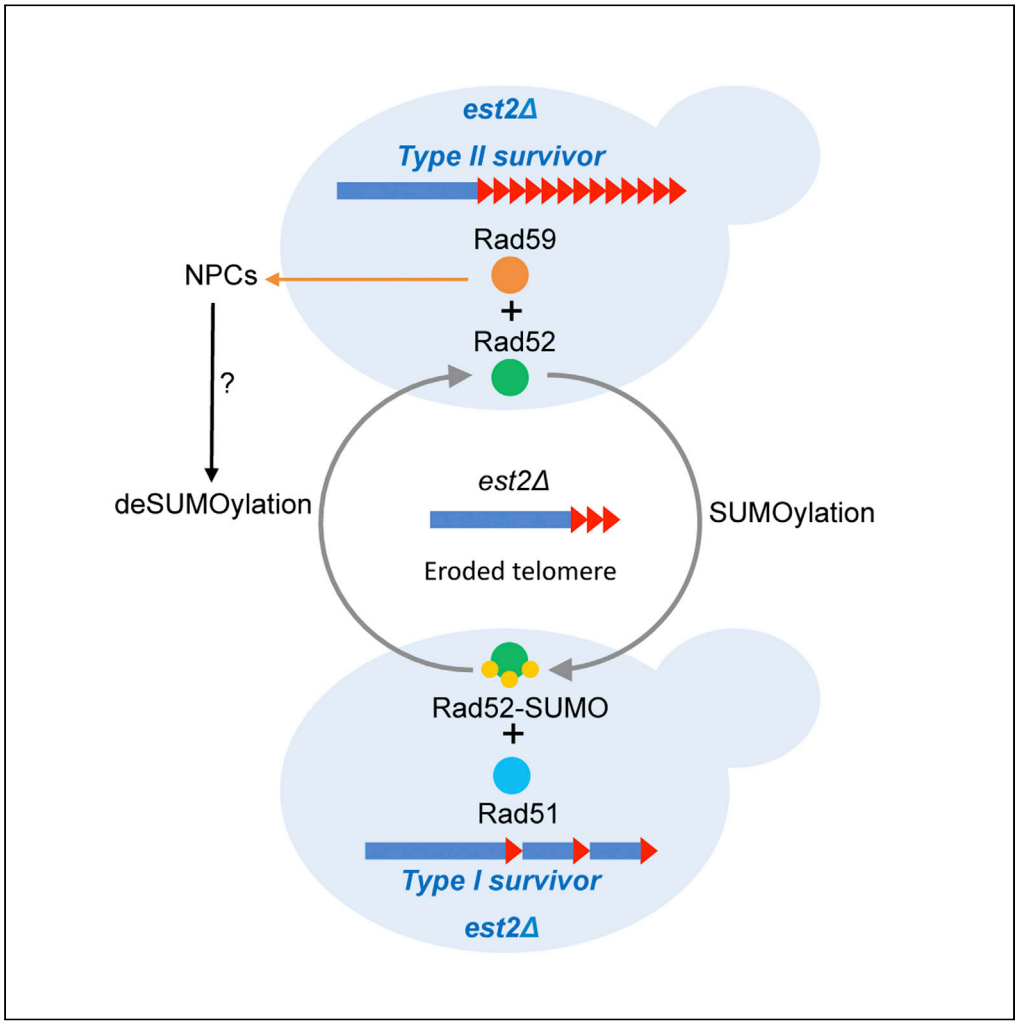

Ferose Charifi, Dmitri Churikov, Nadine Eckert-Boulet, ..., Michael Lisby, Marie-Noëlle Simon, Vincent Géli

marie-noelle.simon@inserm.fr (M.-N.S.)
vincent.geli@inserm.fr (V.G.)

HIGHLIGHTS

RPA SUMOylation is dispensable for *est2Δ* type II survivor formation

Rad52 SUMOylation promotes Rad51-dependent type I survivor pathway

Rad52 deSUMOylation shifts the balance in favor of type II survivor formation

Rad59 is required for relocalization of eroded telomeres to the Nuclear Pore complex

Charifi et al., iScience *24*, 102231
March 19, 2021
https://doi.org/10.1016/j.isci.2021.102231

iScience

CellPress
OPEN ACCESS

Article

Rad52 SUMOylation functions as a molecular switch that determines a balance between the Rad51- and Rad59-dependent survivors

Ferose Charifi,[1,3] Dmitri Churikov,[1,3] Nadine Eckert-Boulet,[2] Christopher Minguet,[1] Frédéric Jourquin,[1] Julien Hardy,[1] Michael Lisby,[2] Marie-Noëlle Simon,[1,*] and Vincent Géli[1,4,*]

SUMMARY

Functional telomeres in yeast lacking telomerase can be restored by rare Rad51- or Rad59-dependent recombination events that lead to type I and type II survivors, respectively. We previously proposed that polySUMOylation of proteins and the SUMO-targeted ubiquitin ligase Slx5-Slx8 are key factors in type II recombination. Here, we show that SUMOylation of Rad52 favors the formation of type I survivors. Conversely, preventing Rad52 SUMOylation partially bypasses the requirement of Slx5-Slx8 for type II recombination. We further report that SUMO-dependent proteasomal degradation favors type II recombination. Finally, inactivation of Rad59, but not Rad51, impairs the relocation of eroded telomeres to the Nuclear Pore complexes (NPCs). We propose that Rad59 cooperates with non-SUMOylated Rad52 to promote type II recombination at NPCs, resulting in the emergence of more robust survivors akin to ALT cancer cells. Finally, neither Rad59 nor Rad51 is required by itself for the survival of established type II survivors.

INTRODUCTION

Telomeres are nucleoprotein structures located at the chromosome ends. They ensure complete replication of and prevent undesirable repair activities at the chromosome physical ends (Kupiec, 2014). In *Saccharomyces cerevisiae*, telomeres form perinuclear foci, the formation of which depends on two redundant pathways that involve Sir4 and the heterodimeric yKu70-yKu80 complex (Taddei et al., 2004). Sir4 anchors telomeres to the nuclear membrane via its interaction with the nuclear-membrane-associated Esc1 (Andrulis et al., 2002; Gartenberg et al., 2004; Taddei et al., 2004), whereas yKu-dependent anchoring has different requirement in G1 and S-phase. In G1, it depends on yKu70 and on a yet unidentified membrane factor, whereas in S-phase it requires the telomerase holoenzyme and the integral nuclear membrane protein Mps3 that also contributes to the Sir4-dependent anchoring (Bupp et al., 2007; Oza et al., 2009; Schober et al., 2009; Taddei et al., 2010). In normal conditions, perinuclear positioning of telomeres is regulated by the covalent attachment of the small ubiquitin-like modifier (SUMO/Smt3). SUMOylation of both Yku70/80 and Sir4 by the SUMO E3 ligase Siz2 promotes telomere anchoring to the nuclear envelope (NE) (Ferreira et al., 2011). Telomere recombination is normally repressed, and their peripheral positioning may sequester telomeres in an HR-inhibitory zone (Géli and Lisby, 2015).

In the absence of telomerase, telomeres progressively shorten with each cell division until their protective function fails. At this point, the cell population enters irreversible growth arrest (Lundblad and Szostak, 1989) often referred to as replicative senescence. In addition, telomerase-negative cells may undergo stochastic reversible arrests, consistent with the repair of accidental telomere damage probably arising as a result of telomere replication stress due to absence of telomerase (Aguilera et al., 2020; Churikov et al., 2014; Simon et al., 2016; Xie et al., 2015; Xu et al., 2015). Crisis is defined as the time point when most of the cells in a population are arrested at the G2/M transition (or dead). This arrest results from activation of the Mec1-dependent DNA damage checkpoint that is activated directly in response to deprotected telomeres (Enomoto et al., 2002; Hector et al., 2012; IJpma and Greider, 2003). Rare survivors are able to escape the permanent arrest by repairing their telomeres via two distinct pathways that require both the essential homologous recombination factor Rad52 and the non-essential subunit of DNA polymerase δ, Pol32 (Chen et al., 2001; Lundblad and Blackburn, 1993; Lydeard et al., 2010). Type I survivors depend on

[1]Marseille Cancer Research Center (CRCM), U1068 Inserm, UMR7258 CNRS, Aix Marseille University, Institut Paoli-Calmettes, Marseille, 13009, France

[2]Department of Biology, University of Copenhagen, Copenhagen N, Denmark

[3]These authors contributed equally

[4]Lead contact

*Correspondence: marie-noelle.simon@inserm.fr (M.-N.S.), vincent.geli@inserm.fr (V.G.)

https://doi.org/10.1016/j.isci.2021.102231

Rad51 and exhibit amplified subtelomeric Y′ elements and short terminal telomeric sequences (Le et al., 1999). Type II survivors display long heterogeneous terminal TG_{1-3} sequences and their formation requires the MRX complex, Rad59, the yeast RecQ helicase Sgs1, and Sae2 (Chen et al., 2009; Hardy et al., 2014; Le et al., 1999; Lee et al., 2007; Teng et al., 2000). In liquid cultures, type I survivors appear first, but the cultures are quickly taken over by type II survivors that have nearly wild-type growth rate (Hardy et al., 2014; Teng and Zakian, 1999).

As telomeres shorten, they lose their capping function and are subject to unregulated degradation by nucleases (Dewar and Lydall, 2012; Hardy et al., 2014). Accordingly, the amount of single-stranded DNA increases at telomeres during senescence (Deshpande et al., 2011; Fallet et al., 2014), and RPA is increasingly recruited to telomeres in senescing cells (Khadaroo et al., 2009). We previously reported that eroded telomeres relocalize from the nuclear envelope to the nuclear pore complex (Khadaroo et al., 2009). We further showed that eroded telomeres accumulate high level of SUMOylated telomere bound proteins that are recognized by the SUMO-targeted ubiquitin ligase (STUbL) Slx5-Slx8 (Churikov et al., 2016). Relocation to the NPCs appears to be causally linked to the recruitment of Slx5-Slx8 to eroded telomeres (Churikov et al., 2016). This process shares similarities with the relocation of irreparable DSBs and expanded CAG repeats to the NPCs (Horigome et al., 2016; Nagai et al., 2008; Su et al., 2015) but may also exhibit some differences. We and others proposed that failure to repair telomeres via canonical HR leads to excessive accumulation of SUMO, which targets telomeres to the NPCs where recombination intermediates can be stripped of SUMOylated proteins (Géli and Lisby, 2015; Nagai et al., 2011). In turn, this would help to disassemble dead-end recombination intermediates, thus allowing type II telomere recombination as a telomere rescue pathway (Freudenreich and Su, 2016; Géli and Lisby, 2015).

DNA damage triggers a SUMOylation wave promoted by extended ssDNA that results in the SUMOylation of a whole set of DNA damage checkpoint, replication, and repair proteins (Burgess et al., 2007; Cremona et al., 2012; Psakhye and Jentsch, 2012; Sacher et al., 2006). The SUMOylation of individual homologous recombination proteins are thought to act synergistically through a combination of SUMO-SIM interactions to accelerate DNA repair (Psakhye and Jentsch, 2012). In addition, a number of constitutive telomeric proteins are also SUMOylated including yKu, Rap1, and Cdc13 (Hang et al., 2014; Lescasse et al., 2013), and we previously showed that Rfa1 is SUMOylated in response to telomere erosion in *est2Δ* cells (Churikov et al., 2016). In this study, we address the functional consequences of the SUMOylation of RPA and Rad52, two factors essential for telomere recombination. We show that SUMOylation of Rad52 functions as a molecular switch that channels telomere recombination to either Rad51- or Rad59-dependent pathways, revealing a new role of SUMOylation in the choice of the pathway that leads to telomerase-independent survivors. We further show that relocation of the eroded telomeres to the NPCs is greatly impaired in the absence of the Rad52 paralog Rad59, suggesting that specific recombination intermediates play a role in the tethering of eroded telomeres to the NPC.

RESULTS

SUMOylation-deficient RPA still interacts with STUbL Slx5-Slx8 and *rfa-5KR* cells form type II survivors in the absence of telomerase

We previously reported that the SUMOylation state of proteins bound to telomeres is a key determinant in the spatial regulation of telomere recombination (Churikov et al., 2016). We demonstrated that RPA physically interacts with the Slx5/Slx8 STUbL and that polySUMOyalted forms of RPA accumulate during senescence in the absence of STUbL activity. To further elucidate the role of RPA SUMOylation, we mutated five lysines distributed over the three subunits of RPA, which were reported to be the major SUMOylation sites (Psakhye and Jentsch, 2012). The resulting mutant, *rfa1-K133R,K170R,K427R rfa2-K199R rfa3-K46R* (*rfa-5KR* henceforth), showed reduced SUMOylation in response to methyl-methane sulfonate (MMS) exposure (Figure 1A). Notably, the *rfa-5KR* mutant still co-immunoprecipitated with Slx5 (Figure 1B), suggesting that the basal interaction between the two proteins is largely independent of SUMO-SIM binding. We next assessed the type of survivors generated in the *rfa-5KR* background in the absence of telomerase. A heterozygous *EST2/est2Δ RFA/rfa-5KR* diploid strain was sporulated, and tetrads were dissected. After the germination of the spores (20–30 generations), telomerase negative cells were selected, inoculated in liquid culture, and propagated by diluting to OD_{600} = 0.1 every 24 h. To avoid any bias in the starting length of telomeres, *est2Δ* and *est2Δ rfa-5KR* clones were isolated from the same diploid. As expected, proliferation of the *est2Δ* cells progressively declined, culminating in the crisis after about 70 population doublings (PDs) when most of the cells stopped dividing before type II survivors took over the culture (Figures 1C and

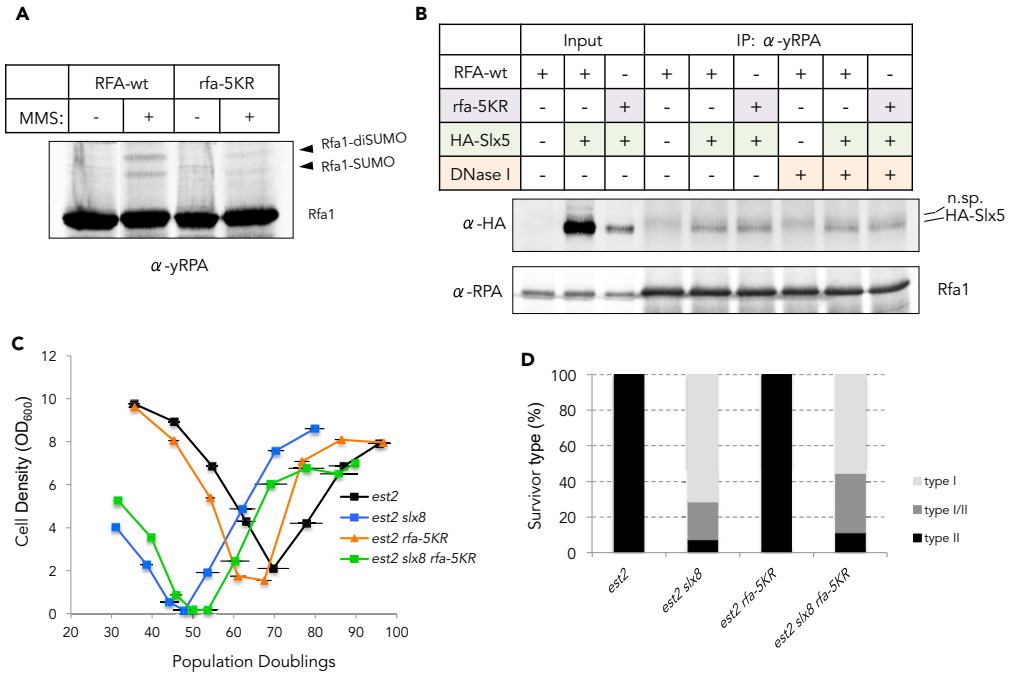

Figure 1. SUMOylation-deficient RPA mutant retains basal interaction with Slx5 and does not affect type II survivor formation

(A) The effect of *rfa-5KR* mutation on MMS-induced Rfa1 SUMOylation was analyzed by immunoblotting with anti-RFA serum. The cells were treated with 0.25% MMS for 2 h where indicated.

(B) Co-immunoprecipitation of the HA-Slx5 with either Rfa1 wild-type or Rfa-5KR proteins. The presence of HA-Slx5 in the anti-RPA immunoprecipitates was determined by anti-HA (12CA5) immunoblotting. The fuzzy band detected in all anti-RPA immunoprecipitates is due to cross-reactivity of the anti-HA antibody with unknown protein precipitating with anti-RPA serum. To verify DNA-independent interaction between HA-Slx5 and Rfa1, the extracts were treated with DNase I (100 μg/mL) for 30 min on ice prior to immunoprecipitation.

(C) Mean senescence profiles of *est2Δ* (n = 12), *est2Δ slx8Δ* (n = 8), *est2Δ rfa-5KR* (n = 17), and *est2Δ rfa-5KR slxΔ8* (n = 9) clones. Each clone issued from a spore colony was propagated in liquid culture through daily serial dilution. OD_{600} was measured every day to estimate the cell density reached in 24 h. PD numbers were estimated from the initial spores. Bars are SD.

(D) Relative frequencies of the telomerase-independent survivor types formed by the clones analyzed in (C). Note that the profile of *est2Δ slx8Δ* is from a total of 28 clones that have been analyzed throughout this study (see also Figure 4).

1D). The *rfa-5KR* slightly accelerated senescence of *est2Δ* cells, indicating that RPA SUMOylation facilitates telomere maintenance early after inactivation of telomerase. Yet, we did not find any defect in the ability of *rfa-5KR* mutant to form type II survivors in liquid cultures (Figures 1C and 1D). We reasoned that if type II recombination requires either degradation or deSUMOylation of poly-SUMOylated RPA at the nuclear pores, we may expect SUMOylation-defective RPA mutant to bypass the necessity of NPC relocalization. To address this possibility, we analyzed the type of survivors produced by *est2Δ rfa-5KR* cells carrying a deletion of *SLX8* that prevents relocalization of eroded telomeres to the NPCs (Churikov et al., 2016). We found that the *rfa-5KR* allele slightly delayed the senescence of *est2Δ slx8Δ* cells (Figure 1C) and moderately rescued type II recombination in *slx8Δ* cells (Figure 1D). The lack of complete rescue of the type II recombination in the absence of STUbL activity by the SUMOylation-defective RPA suggested that Slx5-Slx8 targets other poly-SUMOylated proteins in which efficient turnover and/or de-SUMOylation is required for full-capacity type II recombination.

Because we found that RPA SUMOylation is dispensable for basal interaction between Slx5 and RPA, we tested whether type II recombination depends on efficient binding of RPA to the telomeres. To this end, we took advantage of the *rfa1-D228Y* allele (Smith and Rothstein, 1995). The RPA-D228Y complex shows reduced affinity for single-stranded DNA *in vitro* (Audry et al., 2015; Deng et al., 2014) and elevated level of recombination *in vivo* (Smith and Rothstein, 1999). After sporulation of a heterozygous *EST2/est2Δ RFA1/rfa1-DD28Y* diploid and selection of the appropriate genotypes, senescence rate and survivor

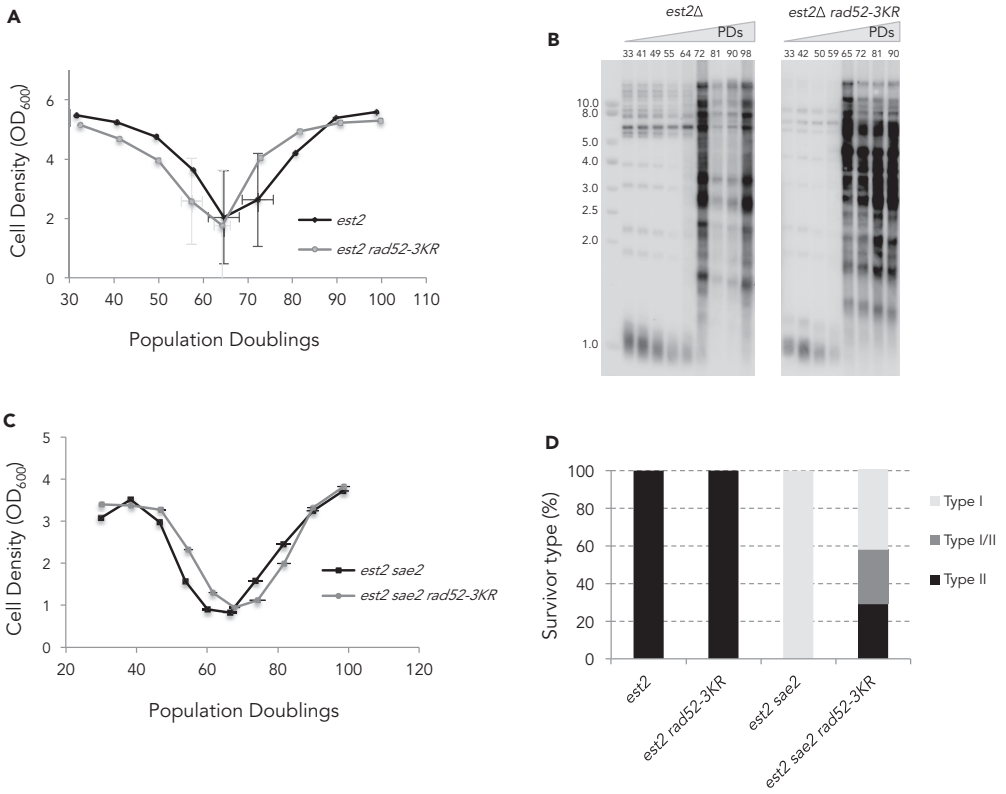

Figure 2. The absence of Rad52 SUMOylation accelerates replicative senescence and facilitates type II survivor formation

(A) Mean replicative senescence curves of *est2Δ* and *est2Δ rad52-3KR* (n = 26). Error bars are SDs.

(B) Telomere length and recombination were analyzed by TG_{1-3} probed Southern blot of *XhoI*-digested DNA prepared from samples of the replicative senescence. The result for two representative clones is shown. The number of PDs from spore germination is indicated.

(C) Mean senescence profiles of *est2Δ saeΔ* (n = 4), *est2Δ* and *est2Δ rad52-3KR* (n = 7) clones.

(D) Relative frequencies of the telomerase-independent survivor types for *est2Δ* (n = 44), *est2Δ rad52-3KR* (n = 26), *est2Δ sae2Δ* (n = 4), and *est2Δ sae2Δ rad52-3KR* (n = 7) clones.

production were analyzed as described earlier. The Figures S1A–S1C shows that *rfa1-D228Y* greatly accelerated senescence and prevented the formation of type II survivors in four out of four independent clones analyzed. Together, our data suggest that although high-affinity-binding of RPA is crucial for both preventing precocious senescence and for the formation of type II survivors, its SUMOylation is largely dispensable for type II recombination.

Rad52 SUMOylation influences the balance between telomere recombination pathways

Treatment with genotoxic agents induce mono- and di-SUMOylated forms of Rad52 with apparent molecular masses of approximately 85 and 105 kDa (Sacher et al., 2006). We analyzed Rad52 SUMOylation status in telomerase-negative cells at different stages of senescence obtained by sequential re-streaking on solid medium (Figure S2). We detected two Rad52 forms that migrate as the mono- and di-SUMOylated Rad52 that were also observed in *EST2* positive cells treated with MMS (Figure S2). We concluded that Rad52 became mono- and di-SUMOylated upon telomere erosion and remained SUMOylated in survivors.

We next addressed the role of Rad52 SUMOylation during the course of telomere erosion. Growth rates were analyzed in telomerase-negative cells (*est2Δ*) carrying the *rad52-K43,44,253R* allele (called *rad52-3KR*) encoding a non-SUMOylatable form of Rad52 (Sacher et al., 2006). After sporulation of a heterozygous *EST2/est2Δ RAD52/rad52-3KR* diploid and selection of the appropriate genotypes, senescence rate was analyzed as described earlier. Examination of a large number of independent clones revealed that *rad52-3KR* conferred a slightly accelerated senescence (Figure 2A). Analysis of telomere length indicated

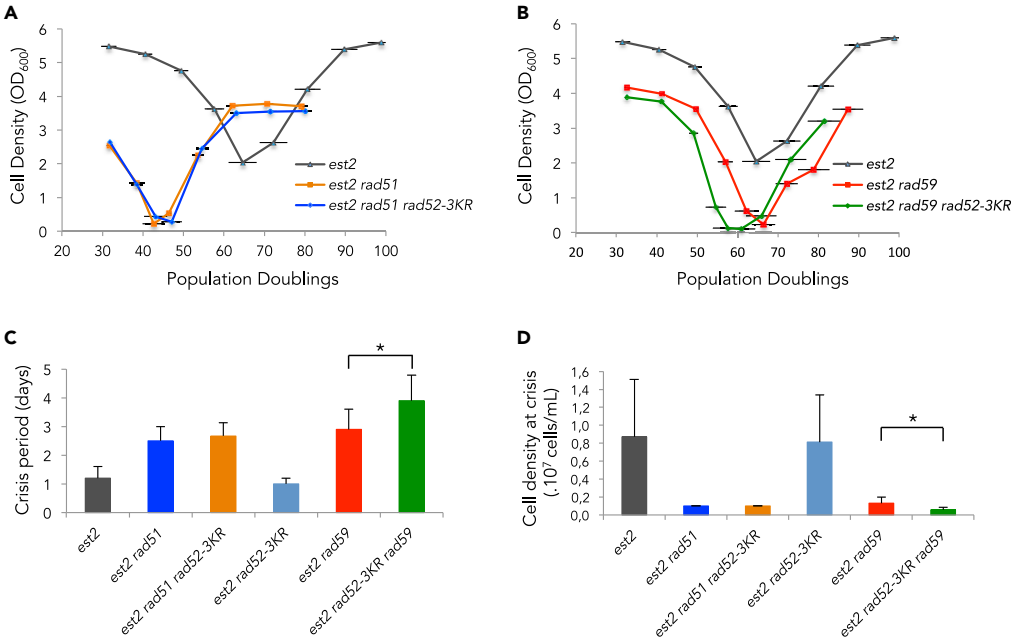

Figure 3. The *rad52-3KR* mutation impairs Rad51-dependent type I survivor formation

(A) Mean replicative senescence curves of *est2Δ*, *est2Δ rad51*Δ (n = 4), and *est2Δ rad51Δ rad52-3KR* (n = 3) cells. Bars are SD.

(B) Replicative senescence *est2Δ*, *est2Δ rad59Δ* (n = 10), and *est2Δ rad59Δ rad52-3KR* (n = 8) clones. Bars are SD.

(C) The crisis period is determined as the number of days the cell population stays arrested for each individual clones analyzed. Crisis period average calculated for each mutant is represented. T test analysis between crisis period of *est2Δ rad59Δ* and *est2Δ rad59Δ rad52-3KR* spores scores 0.029 (*).

(D) Cell density at crisis corresponds to the optical density (OD) at 600nm measured at the nadir of crisis. Average of the lowest OD_{600} during replicative senescence is represented for each mutant. T test analysis between *est2Δ rad59Δ* and *est2Δ rad59Δ rad52-3KR* spores scores 0.016 (*).

that the rate of telomere shortening was similar between *est2Δ* and *est2Δ rad52-3KR* cells (Figure 2B). Next, we aimed to determine the effect of non-SUMOylatable Rad52 on the choice of survivor pathway. Because *est2Δ* cells generate mainly type II survivors in liquid cultures, we introduced the *rad52-3KR* allele *in est2Δ* cells carrying a deletion of *SAE2* that impairs type II survivor formation (Churikov et al., 2014; Hardy et al., 2014). Analysis of several independent *sae2Δ est2Δ rad52-3KR* clones revealed that a number of them generated type II survivors (Figures 2C and 2D), suggesting that non-SUMOylatable Rad52 may favor type II survivor formation. To further address the role of Rad52 SUMOylation in telomere recombination, we combined the *rad52-3KR* mutation with deletions of either *RAD51* or *RAD59*, specifically required for type I and type II survivors formation, respectively (Chen et al., 2001; Le et al., 1999). *est2Δ rad52-3KR rad51Δ* and *est2Δ rad52-3KR rad59Δ* clones were isolated from the suitable heterozygous diploid strains and processed as described earlier (Figure 3). The absence of either Rad51 or Rad59 in telomerase negative cells has been reported to accelerate replicative senescence (Chen et al., 2001; Johnson et al., 2001). As shown in Figures 3A and 3B, preventing the SUMOylation of Rad52 did not affect the kinetics of senescence of *rad51Δ*, whereas it did accelerate senescence of *rad59Δ* cells. In addition, the *est2Δ rad59Δ rad52-3KR* triple mutant exhibited an extended crisis period, indicating that formation of type I survivors was delayed compared with the *est2Δ rad59Δ* double mutant (Figure 3C). Consistent with these results, careful examination of the cell density at crisis indicated that the *rad52-3KR* mutation decreases the survival of the *est2Δ rad59Δ* double mutant (Figure 3D). Collectively, these results indicate that SUMOylation of Rad52 fosters Rad51 functions during senescence, including formation of type I survivors. This inference was reinforced by the analysis of the *rad51* mutant lacking the carboxy-terminal SIM domain that has been shown to strengthen the interaction between Rad51 and SUMOylated Rad52 (Bergink et al., 2013). To determine the ability of the *rad51ΔSIM* allele to sustain Rad51-dependent recombination during senescence, we introduced it in *est2Δ sae2Δ* cells that are impaired in type II survivor formation. We found that the *rad51ΔSIM* accelerated senescence

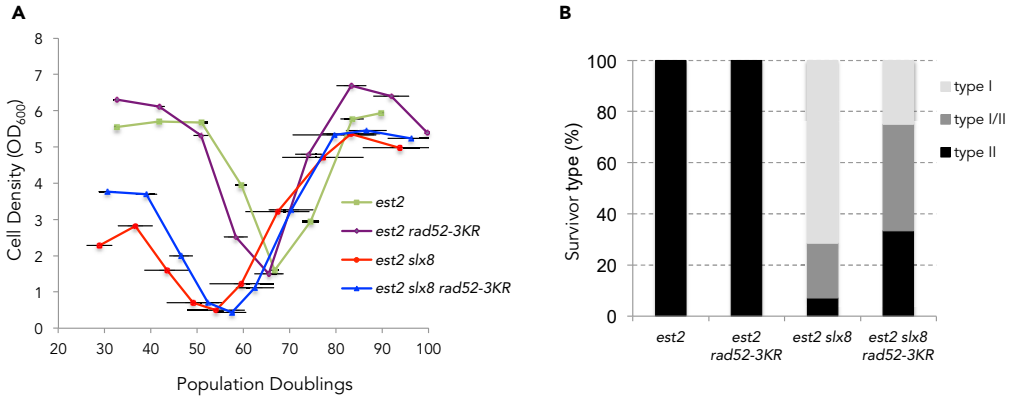

Figure 4. The *rad52-3KR* mutation partially bypasses the need for Slx8 for type II survivor formation

(A) Mean senescence profiles of *est2Δ* (n = 7), *est2Δ slx8Δ* (n = 11), *est2Δ rad52-3KR* (n = 6), and *est2Δ rad52-3KR slxΔ8* (n = 14) clones. The *est2Δ slx8Δ* profile is as in Figure 1D and is shown for comparison. Bars are SD.

(B) Relative frequencies of the telomerase-independent survivor types formed by the clones analyzed in (A).

(Figure S3A) and exhibited a reduced ability to produce type I survivors in the *sae2Δ* background as shown by a prolonged crisis period before survivor appearance (Figure S3A and S3B).

The absence of Rad52 SUMOylation partially bypasses the role of Slx5-Slx8 in type II survivor formation

We previously suggested that deSUMOylation and/or SUMO-dependent degradation of telomere-bound proteins at the nuclear pore might favor type II recombination (Géli and Lisby, 2015). Therefore, our findings that *rad52-3KR* benefits type II recombination suggest that Rad52 might be one of the targets of this deSUMOylation pathway. We thus addressed the possibility that preventing Rad52 SUMOylation bypasses the need for Slx5-Slx8 STUbL activity in type II recombination. To this end, we analyzed the type of survivors produced by *est2Δ rad52-3KR* cells carrying a deletion of *SLX8*. The *rad52-3KR* allele did not significantly rescue the accelerated senescence induced by the absence of Slx8 (Figure 4A). However, the non-SUMOylatable form of Rad52 favored type II recombination even in the absence of STUbL activity as more type II recombination events occurred in *est2Δ slx8Δ rad52-3KR* as compared with *est2Δ slx8Δ* cells (Figure 4B, p = 0,01). This suggests that deSUMOylation or degradation of SUMO-Rad52 at the NPC could be one link that connects type II recombination with relocalization of eroded telomeres to the NPCs.

SUMO-dependent proteasomal degradation promotes type II recombination

The ATPase Cdc48 facilitates extraction from chromatin of the proteins marked by ubiquitin or SUMO for degradation by the proteasome. It acts together with the substrate-recruiting co-factor Ufd1 that binds SUMOylated proteins and operates as a selective receptor for STUbL targets (Nie et al., 2012). Because Cdc48/Ufd1 binds to SUMOylated Rad52 and acts in parallel with Srs2 in restricting Rad51 levels on DNA (Bergink et al., 2013), we investigated whether it impacts type II recombination. We isolated *est2Δ* clones carrying either the temperature-sensitive allele *ufd1-2* or an allele of *ufd1* lacking the C-terminal SIM domain (*ufd1Δ SIM*) and monitored their senescence profiles at 30°C. Both alleles appeared to slightly accelerate senescence and extend the crisis period, suggesting that fully functional Cdc48/Ufd1 complexes are required for survivor formation (Figures 5A and 5B). Telomere length analysis by Southern blot further showed that the mutant alleles of *UFD1* preferentially impact or delay the appearance of type II survivors (Figures 5C and S5). In line with the observation that Cdc48/Ufd1 weakens the Rad51-Rad52 interaction through its binding to SUMOylated Rad52 (Bergink et al., 2013; Niu and Klein, 2017), this result further supports our hypothesis that shifting a balance of Rad52 interactions from Rad51 toward Rad59 allows the telomeres to engage in type II recombination. It also suggested that formation of the Rad51 filament at eroded telomeres may impede type II recombination.

Because Srs2 has the ability to both dismantle and prevent re-formation of Rad51 filament, we next tested whether this protein is required for type II recombination. The deletion of *SRS2* did not significantly impact the rate of senescence (Figure S6A) but completely prevented formation of type II survivors as five out of five independent *est2Δ srs2Δ* clones formed only type I survivors in liquid cultures (Figure S6B). Because

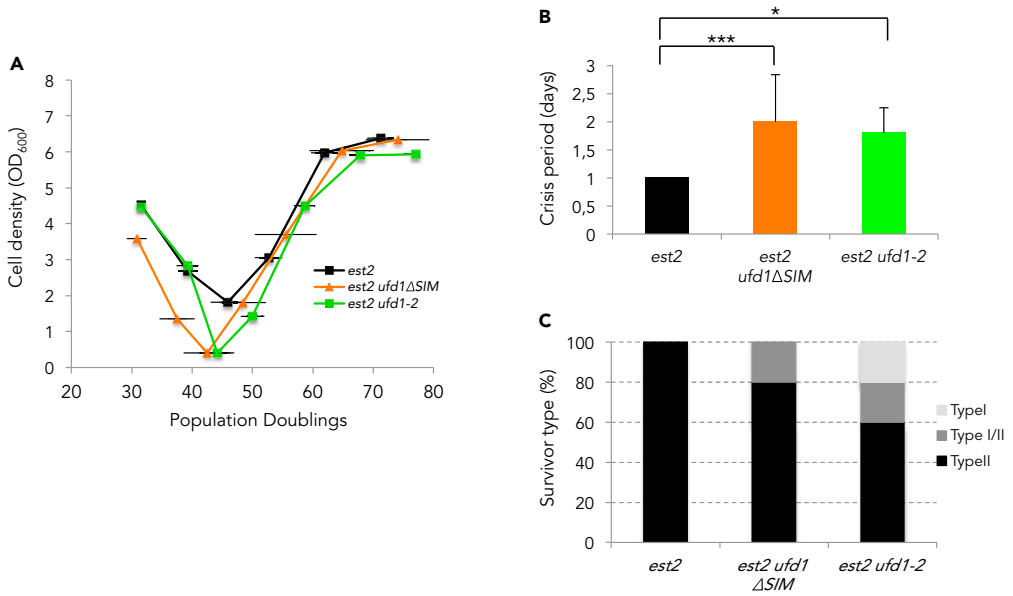

Figure 5. Ufd1 mutants impact type II recombination

(A) Mean replicative senescence curves of *est2Δ* (*n = 6*), *est2Δ ufd1*ΔSIM (n = 6), and *est2Δ ufd1-2* (n = 6) cells. Bars are SD.

(B) Average of the length of the crisis period for each mutant is represented (see Figure 3C). Statistical differences were determined by a Fisher's exact test (*p = 0.022, ***p = 0.008).

(C) Relative frequencies of the telomerase-independent survivor types formed.

Srs2 is a multi-functional protein (Figure S6C), we took advantage of the well-characterized Srs2 C-terminal truncation mutants (Niu and Klein, 2017) to ask which of its functions is instrumental for type II recombination. One mutant, *srs2* 1–998, retains both the helicase and Rad51 displacement activity but is missing the PCNA interaction domain and the other, *srs2* 1–860, lacks in addition to the Rad51 interaction domain. Neither mutant affected type II recombination (Figure S6D). This suggests that the helicase function of Srs2 rather than its strippase activity is required for type II recombination. From these experiments, we conclude that Srs2 rather functions in the break-induced replication that generates long telomeres in type II survivors in line with its role in preventing toxic structures during BIR (Elango et al., 2017).

Rad59, but not Rad51, is required to target eroded telomeres to the NPC

To further explore the requirements for telomere localization to NPCs, we used fluorescence microscopy to address the role of DNA repair proteins in this process. As previously described, to monitor telomere relocalization to NPCs we used the *est2*Δ p*EST2-URA3* strain carrying an N-terminal deletion of Nup133 (*nup133ΔN*) and expressing *CDC13-YFP*, *RAD52-RFP*, and *CFP-NUP49* under the control of their native promoters (Khadaroo et al., 2009). The *nup133ΔN* causes NPC clustering at one side of the nucleus. After loss of telomerase, the position of eroded telomeres were determined by the colocalization of Cdc13-YFP, Rad52-RFP foci, and CFP-Nup49 as cells progressed into senescence (Figure 6A) (Churikov et al., 2016; Khadaroo et al., 2009). In agreement with our previous studies, we observed that Cdc13-YFP and Rad52-RFP colocalized in a single focus at the NPC cluster after loss of telomerase (Figure 6A). The *rfa-5KR* mutations only partially affected the relocation of eroded telomeres to the NPC (Figure 6B). We next analyzed telomere relocation to the NPC in cells lacking either Rad59 or Rad51. The absence of Rad51 did not prevent the relocalization of eroded telomeres to the NPC (Figure 6B) and in fact slightly augmented it. In striking contrast, deletion of *RAD59* largely abolished the Cdc13-YFP and Rad52-RFP colocalization with the NPC (Figure 6C).

Because Rad59 is also SUMOylated at lysines 207 and 228 in response to DNA damage (Psakhye and Jentsch, 2012; Silva et al., 2016), we asked whether a non-SUMOylatable allele of *RAD59* (*rad59-K207,228R* a.k.a. *rad59-2KR*) would affect telomere localization and recombination. Telomerase negative cells carrying the *rad59-2KR* allele exhibited a slightly delayed senescence (Figure S7A). Similarly to *est2Δ* cells, the *est2Δ rad59-2KR* cells produced type II survivors in liquid culture (Figure S7B), indicating

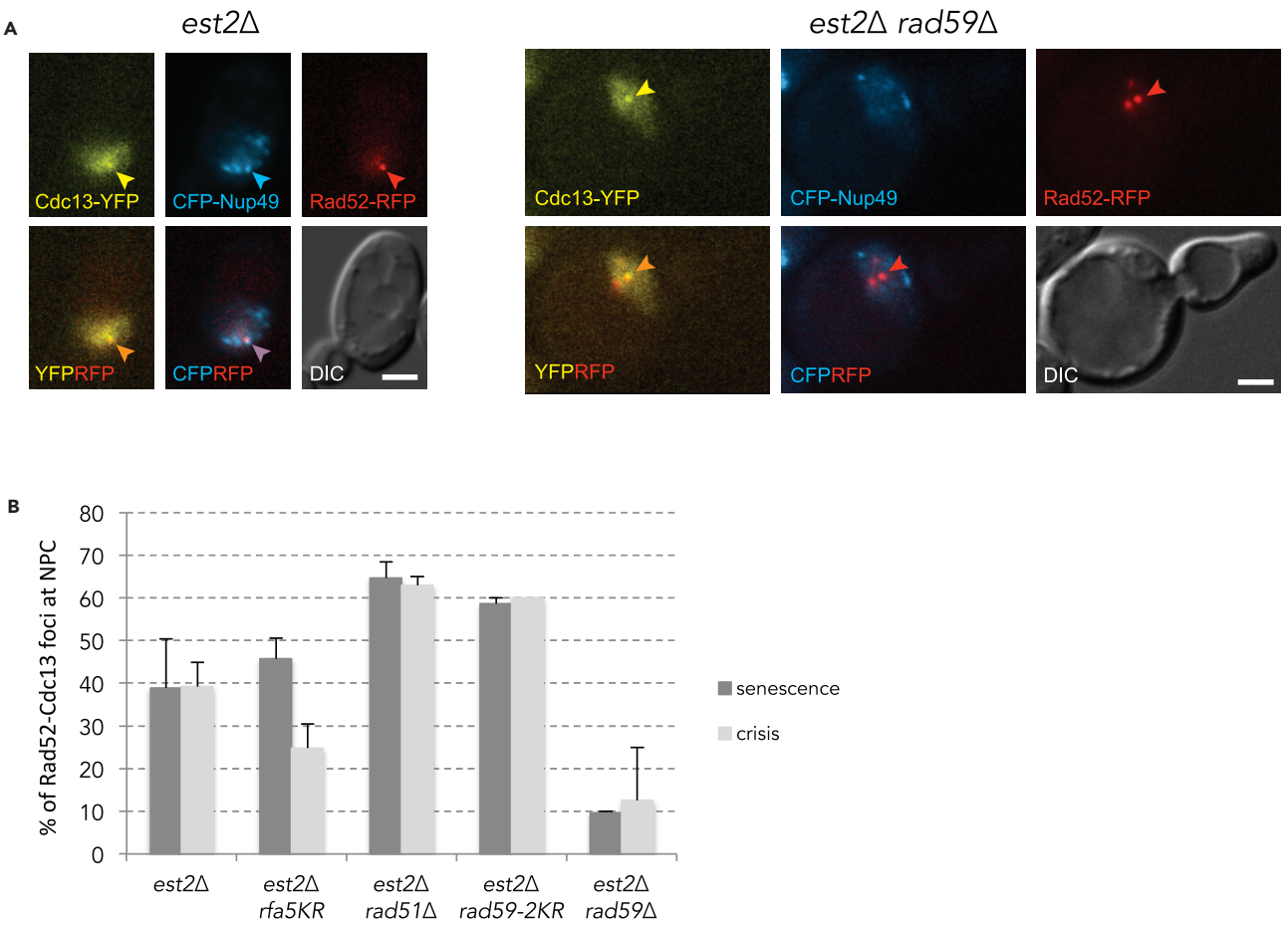

Figure 6. Rad59, but not Rad51, is required to tether eroded telomeres at the NPC

(A) Co-localization of Cdc13-YFP/Rad52-RFP foci with CFP-Nup49 during replicative senescence in *est2Δ* cells. Eroded telomeres in *est2Δ* cells are detected as foci containing both Rad52-RFP and Cdc13-YFP in the *nup133ΔN* background, which causes Nup49-CFP (NPCs) to cluster at one side of the nucleus. Representative images illustrating the colocalization of Cdc13, Rad51, and Nup49 are shown.

(B) Quantification of the triple colocalization of Cdc13-YFP, Rad52-RFP, and Nup49-CFP during senescence and at the time of crisis. The data are represented as the means ± SEM for 4, 2, 4, 2, and 2 biological replicates for the *est2Δ*, *est2 rfa1-5KR*, *est2Δ rad51Δ*, *est2Δ rad59-2KR*, *and est2Δ rad59Δ* mutants, respectively. Control *est2Δ* are from Churikov et al., (2016).

that Rad59 SUMOylation has no detectable impact on type II recombination. In contrast to *rad59Δ* cells, telomere relocation to the NPC was not affected in the *rad59-2KR* mutant (Figure 6B). We concluded that Rad59 is required for telomere relocalization to and/or stabilization at the NPC independently of its SUMOylation, whereas Rad51 does not seem to be involved in this process. These results draw an intriguing link between the positive role that Rad59 plays in type II survivor pathway and its requirement for relocalization of eroded telomeres to NPCs.

Rad59 is dispensable for telomere maintenance in type II survivors

To determine whether the role of Rad59 extends beyond the initial elongation of telomeres by type II recombination, we asked whether Rad59 is still required for telomere maintenance in the established type II survivors. One *RAD59* allele was deleted in an *est2Δ* diploid strain isolated by crossing type II survivors of opposite mating types. After sporulation of the diploid, the spore colonies were serially restreaked on YPD plates for an estimated number of 250 population doublings (10 restreaks). Strikingly, although Rad59 is strictly required for type II survivor formation, it appeared dispensable to sustain their growth and to maintain the long and heterogeneous telomeres characteristic of type II survivors (Figure 7A). Telomere length appeared to be strictly dependent neither on Rad51 once type II survivors have been stably established (Figure 7A) nor on Slx8, Pif1, and Srs2 that play key role in type II survivor formation (Figure 7B). It thus appeared that once long telomeres are formed,

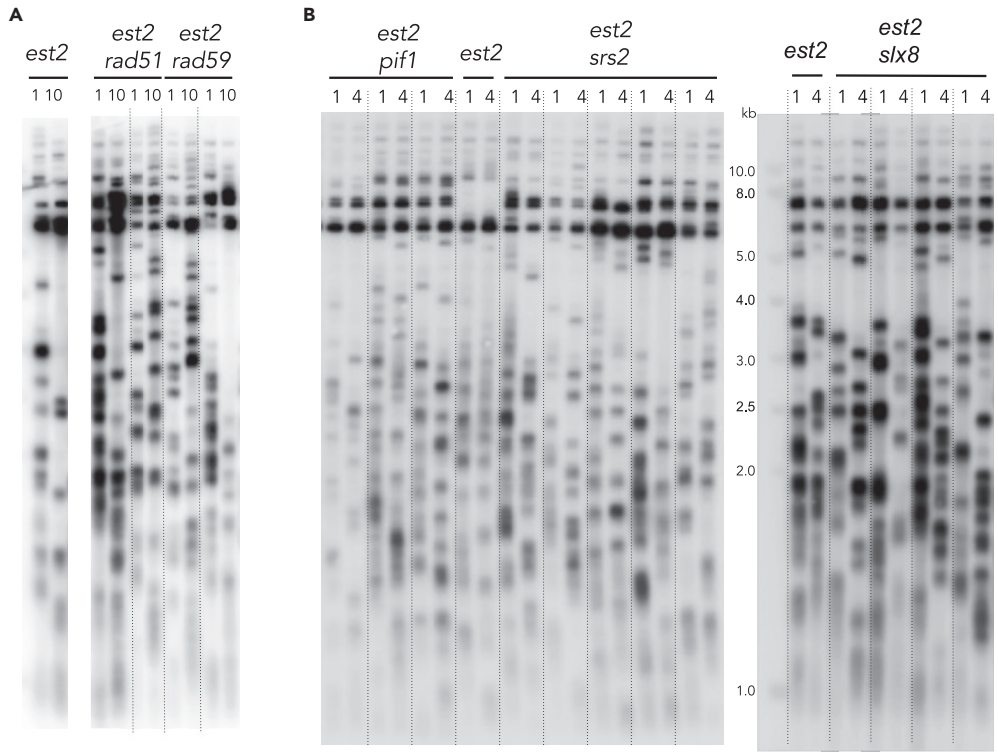

Figure 7. Rad59 is not required for the maintenance of type II survivors

(A) *RAD59* and *RAD51* genes were deleted in an *est2Δ* diploid strain obtained by mating two type II survivors. Haploid type II survivors with the indicated genotypes were obtained after dissection and the spore colonies serially restreaked every two days on YPD plates. The telomere length distribution was analyzed by $TG_{1\text{-}3}$ probed southern blot analysis of DNA isolated at the first and the 10^{th} streak.

(B) A similar approach was used to delete *SRS2*, *SLX8*, and *PIF1* in already formed type II survivors. Telomere length were analyzed as in (A) after 1 and 4 restreaks on plates from independent spore colonies.

several recombination pathways might redundantly ensure repair when a single or few short telomeres arise due to either the end replication problem or accidental telomere breakage.

DISCUSSION

Type I and type II telomere recombination were previously shown to rely on Rad51 and Rad59, respectively (Chen et al., 2001), but what dictates this choice is only partially understood. We have recently shown that type II recombination is linked to relocation of telomeres to the NPC that involves the recognition of telomere-bound SUMOylated proteins by Slx5-Slx8 (Churikov et al., 2016).

In this study, we show that SUMOylation of Rad52 functions as a molecular switch that channels telomere recombination to either Rad51- or Rad59-dependent pathway. Our results indicate that SUMOylation of Rad52 favors Rad51-dependent telomere recombination pathway. This is consistent with the observation that SUMOylation of Rad52 reinforces its interaction with Rad51 (Bergink et al., 2013) and reduces its single-strand annealing activity (Altmannova et al., 2010). We also propose that non-SUMOylatable form of Rad52 may favor Rad59-dependent type II recombination. We show in addition that Rad59 is required to relocate telomeres to the NPC, reinforcing the tight correlation between type II recombination and relocation of eroded telomeres to the NPC (Churikov et al., 2016). We propose that during early stage of senescence, short telomeres with limited levels of single-stranded overhangs and low levels of SUMOylated proteins would be repaired by recombination between subtelomeric Y′ elements or internal $TG_{1\text{-}3}$ tracts that relies on the interaction between SUMO-Rad52 and the SIM domain of Rad51. At later stages of senescence and by the time of crisis when the reservoir of $TG_{1\text{-}3}$ sequences is severely depleted, the efficiency of this repair

is diminished, and telomeres accumulate in the form of "congested" recombination intermediates (Géli and Lisby, 2015). These non-repairable telomeres are then targeted to the NPC through a process involving SUMO and Slx5-Slx8 as well as Rad59.

It has been proposed that STUbL- and NPC-associated Ulp1 both contribute to clean up of the SUMOylated proteins, thereby disassembling dead-end intermediates at resected telomeres (Churikov et al., 2016; Nagai et al., 2011). It is conceivable that deSUMOylation of Rad52 occurs at the NPC and thereby triggers subsequent type II telomere recombination. Although RPA SUMOylation is a key determinant of the relocation of stalled replication forks (Whalen et al., 2020), it appeared largely dispensable for both relocation of eroded telomeres to the NPC and type II recombination. This might be expected if multiple SUMOylated proteins at telomeres interact with Slx5-Slx8, so that preventing SUMOylation of any one of them would have only negligible effect on relocation to NPCs and type II recombination. Furthermore, non-SUMOylatable RPA (rfa-5KR) still interacts with Slx5, suggesting that SUMOylation of RPA might become instrumental only when resection is limited.

The mechanism by which Rad59 contributes to the relocation of eroded telomeres to the NPC remains to be clarified. Recently, Rad59 has also been implicated in the relocation to the NPC of replication forks stalled at long CAG-triplet repeats (Whalen and Freudenreich, 2020; Whalen et al., 2020). Both Rad59 (Davis and Symington, 2003) and Slx5-Slx8 (Churikov et al., 2016) interact with RPA. Whether Rad59 participates in the same pathway of eroded telomeres relocation to NPCs that involves RPA and the Slx5-Slx8 complex or acts independently remains to be determined. One can also envision that the absence of Rad59 channels all telomere recombination to the Rad51-mediated pathway and thus prevents relocalization of the eroded telomeres to the NPC. In support of this notion, deletion of *RAD51* that abolishes the type I recombination pathway did not have any effect on NPC localization. Indeed, *rad59Δ* cells are proficient in the formation of Rad51-dependent type I survivors despite their defect in relocalization of eroded telomeres to the NPCs, indicating that Rad51-dependent recombination does not take place at the NPC. Alternatively, certain Rad59-dependent recombination intermediates may need to be formed at telomeres to induce or stabilize their interaction with NPCs. In line with this possibility, it has recently been shown in *Schizosaccharomyces pombe* that replication forks arrested at a specific replication fork barrier (RFB) relocate to the NPC only when processed by resection factors and recombinase (Kramarz et al., 2020).

Previous studies have shown that Rad59 is endowed with ssDNA annealing activity and interacts with Rad52 likely forming heteromeric rings (Cortés-Ledesma et al., 2004; Davis and Symington, 2003; Silva et al., 2016; Wu et al., 2006). Rad59 has also been shown to physically interact with the ATP-dependent chromatin remodeler RSC (Oum et al., 2011), which is required to maintain proper NPC localization (Titus et al., 2010). It is thus possible that relocation of eroded telomeres to the NPC involves RSC-dependent chromatin remodeling events. Binding of eroded telomeres to the NPC would therefore have different requirements compared with the localization of persistent DSBs to the nuclear envelope that requires the chromatin remodeler INO80, the recombinase Rad51, and SWR1-dependent incorporation of Htz1 (Horigome et al., 2014). This underscores that seemingly conserved process of DNA damage localization to NPC is nevertheless context dependent and is driven by damage-specific mechanisms.

Our data show that Rad59 is only required for the initial formation of type II survivors but not to sustain their growth. As type II survivors arise at crisis when most of the telomere repeats have been lost, it is possible that the initial elongation of telomeres requires a specific Rad59-dependent structure, which is no longer required once a sufficient reservoir of telomeric repeats has been accumulated in the established type II survivors. At that point, several recombination pathways probably can take place to repair either accidental or gradually shortened telomeres arising during successive cell cycles. The redundancy of repair pathways might thus render NPC localization less crucial to maintain the telomeres of type II survivors.

Limitations of the study

Because type II survivors dominate in the liquid cultures of telomerase negative yeast, it is difficult to impossible to demonstrate further enhancement of the type II pathway. For this reason, we used *sae2Δ* background in which resection of the DSBs and eroded telomeres is attenuated, and as a result, the rate of type II survivor formation is diminished giving the opportunity to type I survivors to dominate the cultures. In this background we could demonstrate that non-SUMOylatable Rad52 shifted the balance toward type II

survivors in spite of the structural hindrance to DNA end resection. We cannot rule out however that this is mediated by a negative effect of the non-SUMOylatable Rad52 on type I formation. Although, that would lead to aggravation of the crisis which is not the case. Further work will be needed to clarify when and where Rad52 is deSUMOylated.

Resource availability

Lead contact

Further information and requests for resources and reagents should be directed to and will be fulfilled by the lead contact, Vincent Géli (vincent.geli@inserm.fr).

Materials availability

All materials generated in this study are available upon request. The data that support the findings of the current study are available from the corresponding authors on request.

Data and code availability

No codes.

METHODS

All methods can be found in the accompanying transparent methods supplemental file.

SUPPLEMENTAL INFORMATION

Supplemental information can be found online at https://doi.org/10.1016/j.isci.2021.102231.

ACKNOWLEDGMENTS

We are grateful to Steven Bergink and S. Jentsch for the *rad51ΔSIM, ufd1ΔSIM and ufd1-2* mutants and to H. Klein for *SRS2* mutant strains. VG is supported by the Ligue Nationale Contre le Cancer (équipe labellisée). CM was supported by l'Institut National du Cancer, « PLBIO14-012 ». MNS is supported by the Agence Nationale de la Recherche (ANR-19-CE12-0023 NIRO). ML and NEB were supported by Danish Council for Independent Research, the Villum Foundation, and by the European Research Council (ERCStG, no. 242905).

AUTHOR CONTRIBUTIONS

FC contributed to Figures 2, 3, and S7; DC contributed to Figures 1 and 5; NEB and ML contributed to Figures 6 and S7; FJ contributed to Figures 5 and S3, CM contributed to Figures 1 and S6; JH contributed to Figure 3, MNS contributed to Figures 4, 7, S1, and S2. DC, MNS, and VG wrote the manuscript.

DECLARATION OF INTERESTS

The authors declare no competing interests.

Received: December 3, 2020
Revised: February 1, 2021
Accepted: February 22, 2021
Published: March 19, 2021

REFERENCES

Aguilera, P., Whalen, J., Minguet, C., Churikov, D., Freudenreich, C., Simon, M.-N., and Géli, V. (2020). The nuclear pore complex prevents sister chromatid recombination during replicative senescence. Nat. Commun. *11*, 160.

Altmannova, V., Eckert-Boulet, N., Arneric, M., Kolesar, P., Chaloupkova, R., Damborsky, J., Sung, P., Zhao, X., Lisby, M., and Krejci, L. (2010). Rad52 SUMOylation affects the efficiency of the DNA repair. Nucleic Acids Res. *38*, 4708–4721.

Andrulis, E.D., Zappulla, D.C., Ansari, A., Perrod, S., Laiosa, C.V., Gartenberg, M.R., and Sternglanz, R. (2002). Esc1, a nuclear periphery protein required for sir4-based plasmid anchoring and partitioning. Mol. Cell. Biol. *22*, 8292–8301.

Audry, J., Maestroni, L., Delagoutte, E., Gauthier, T., Nakamura, T.M., Gachet, Y., Saintomé, C., Géli, V., and Coulon, S. (2015). RPA prevents G-rich structure formation at lagging-strand telomeres to allow maintenance of chromosome ends. EMBO J. *34*, 1942–1958.

Bergink, S., Ammon, T., Kern, M., Schermelleh, L., Leonhardt, H., and Jentsch, S. (2013). Role of Cdc48/p97 as a SUMO-targeted segregase curbing Rad51-Rad52 interaction. Nat. Cell Biol. *15*, 526–532.

Bupp, J.M., Martin, A.E., Stensrud, E.S., and Jaspersen, S.L. (2007). Telomere anchoring at the nuclear periphery requires the budding yeast

Sad1-UNC-84 domain protein Mps3. J. Cell Biol. *179*, 845–854.

Burgess, R.C., Rahman, S., Lisby, M., Rothstein, R., and Zhao, X. (2007). The Slx5-Slx8 complex affects sumoylation of DNA repair proteins and negatively regulates recombination. Mol. Cell. Biol. *27*, 6153–6162.

Chen, Q., Ijpma, A., and Greider, C.W. (2001). Two survivor pathways that allow growth in the absence of telomerase are generated by distinct telomere recombination events. Mol. Cell. Biol. *21*, 1819–1827.

Chen, X.-F., Meng, F.-L., and Zhou, J.-Q. (2009). Telomere recombination accelerates cellular aging in Saccharomyces cerevisiae. PLoS Genet. *5*, e1000535.

Churikov, D., Charifi, F., Simon, M.-N., and Géli, V. (2014). Rad59-Facilitated acquisition of Y′ elements by short telomeres delays the onset of senescence. PLoS Genet. *10*, e1004736.

Churikov, D., Charifi, F., Eckert-Boulet, N., Silva, S., Simon, M.-N., Lisby, M., and Géli, V. (2016). SUMO-dependent relocalization of eroded telomeres to nuclear pore complexes controls telomere recombination. Cell Rep. *15*, 1242–1253.

Cortés-Ledesma, F., Malagón, F., and Aguilera, A. (2004). A novel yeast mutation, rad52-L89F, causes a specific defect in Rad51-independent recombination that correlates with a reduced ability of Rad52-L89F to interact with Rad59. Genetics *168*, 553–557.

Cremona, C.A., Sarangi, P., Yang, Y., Hang, L.E., Rahman, S., and Zhao, X. (2012). Extensive DNA damage-induced sumoylation contributes to replication and repair and acts in addition to the mec1 checkpoint. Mol. Cell *45*, 422–432.

Davis, A.P., and Symington, L.S. (2003). The Rad52-Rad59 complex interacts with Rad51 and replication protein A. DNA Repair (Amst) *2*, 1127–1134.

Deng, S.K., Gibb, B., de Almeida, M.J., Greene, E.C., and Symington, L.S. (2014). RPA antagonizes microhomology-mediated repair of DNA double-strand breaks. Nat. Struct. Mol. Biol. *21*, 405–412.

Deshpande, A.M., Ivanova, I.G., Raykov, V., Xue, Y., and Maringele, L. (2011). Polymerase epsilon is required to maintain replicative senescence. Mol. Cell. Biol. *31*, 1637–1645.

Dewar, J.M., and Lydall, D. (2012). Similarities and differences between "uncapped" telomeres and DNA double-strand breaks. Chromosoma *121*, 117–130.

Elango, R., Sheng, Z., Jackson, J., DeCata, J., Ibrahim, Y., Pham, N.T., Liang, D.H., Sakofsky, C.J., Vindigni, A., Lobachev, K.S., et al. (2017). Break-induced replication promotes formation of lethal joint molecules dissolved by Srs2. Nat. Commun. *8*, 1790.

Enomoto, S., Glowczewski, L., and Berman, J. (2002). MEC3, MEC1, and DDC2 are essential components of a telomere checkpoint pathway required for cell cycle arrest during senescence in Saccharomyces cerevisiae. Mol. Biol. Cell *13*, 2626–2638.

Fallet, E., Jolivet, P., Soudet, J., Lisby, M., Gilson, E., and Teixeira, M.T. (2014). Length-dependent processing of telomeres in the absence of telomerase. Nucleic Acids Res. *42*, 3648–3665.

Ferreira, H.C., Luke, B., Schober, H., Kalck, V., Lingner, J., and Gasser, S.M. (2011). The PIAS homologue Siz2 regulates perinuclear telomere position and telomerase activity in budding yeast. Nat. Cell Biol. *13*, 867–874.

Freudenreich, C.H., and Su, X.A. (2016). Relocalization of DNA lesions to the nuclear pore complex. FEMS Yeast Res. *16*, fow095.

Gartenberg, M.R., Neumann, F.R., Laroche, T., Blaszczyk, M., and Gasser, S.M. (2004). Sir-mediated repression can occur independently of chromosomal and subnuclear contexts. Cell *119*, 955–967.

Géli, V., and Lisby, M. (2015). Recombinational DNA repair is regulated by compartmentalization of DNA lesions at the nuclear pore complex: DNA Lesions at the Nuclear Pore Complex. BioEssays *37*, 1287–1292.

Hang, L.E., Lopez, C.R., Liu, X., Williams, J.M., Chung, I., Wei, L., Bertuch, A.A., and Zhao, X. (2014). Regulation of Ku-DNA association by Yku70 C-terminal tail and SUMO modification. J. Biol. Chem. *289*, 10308–10317.

Hardy, J., Churikov, D., Géli, V., and Simon, M.-N. (2014). Sgs1 and Sae2 promote telomere replication by limiting accumulation of ssDNA. Nat. Commun. *5*, 5004.

Hector, R.E., Ray, A., Chen, B.-R., Shtofman, R., Berkner, K.L., and Runge, K.W. (2012). Mec1p associates with functionally compromised telomeres. Chromosoma *121*, 277–290.

Horigome, C., Bustard, D.E., Marcomini, I., Delgoshaie, N., Tsai-Pflugfelder, M., Cobb, J.A., and Gasser, S.M. (2016). PolySUMOylation by Siz2 and Mms21 triggers relocation of DNA breaks to nuclear pores through the Slx5/Slx8 STUbL. Genes Dev *30*, 931–945.

Horigome, C., Oma, Y., Konishi, T., Schmid, R., Marcomini, I., Hauer, M.H., Dion, V., Harata, M., and Gasser, S.M. (2014). SWR1 and INO80 chromatin remodelers contribute to DNA double-strand break perinuclear anchorage site choice. Mol Cell *55*, 626–639.

IJpma, A.S., and Greider, C.W. (2003). Short telomeres induce a DNA damage response in *Saccharomyces cerevisiae*. Mol. Cell. Biol. *14*, 987–1001.

Johnson, F.B., Marciniak, R.A., McVey, M., Stewart, S.A., Hahn, W.C., and Guarente, L. (2001). The Saccharomyces cerevisiae WRN homolog Sgs1p participates in telomere maintenance in cells lacking telomerase. EMBO J. *20*, 905–913.

Khadaroo, B., Teixeira, M.T., Luciano, P., Eckert-Boulet, N., Germann, S.M., Simon, M.N., Gallina, I., Abdallah, P., Gilson, E., Géli, V., et al. (2009). The DNA damage response at eroded telomeres and tethering to the nuclear pore complex. Nat. Cell Biol. *11*, 980–987.

Kramarz, K., Schirmeisen, K., Boucherit, V., Ait Saada, A., Lovo, C., Palancade, B., Freudenreich, C., and Lambert, S.A.E. (2020). The nuclear pore primes recombination-dependent DNA synthesis at arrested forks by promoting SUMO removal. Nat. Commun. *11*, 5643.

Kupiec, M. (2014). Biology of telomeres: lessons from budding yeast. FEMS Microbiol. Rev. *38*, 144–171.

Le, S., Moore, J.K., Haber, J.E., and Greider, C.W. (1999). RAD50 and RAD51 define two pathways that collaborate to maintain telomeres in the absence of telomerase. Genetics *152*, 143–152.

Lee, J.Y., Kozak, M., Martin, J.D., Pennock, E., and Johnson, F.B. (2007). Evidence that a RecQ helicase slows senescence by resolving recombining telomeres. PLoS Biol. *5*, e160.

Lescasse, R., Pobiega, S., Callebaut, I., and Marcand, S. (2013). End-joining inhibition at telomeres requires the translocase and polySUMO-dependent ubiquitin ligase Uls1. EMBO J. *32*, 805–815.

Lundblad, V., and Blackburn, E.H. (1993). An alternative pathway for yeast telomere maintenance rescues est1- senescence. Cell *73*, 347–360.

Lundblad, V., and Szostak, J.W. (1989). A mutant with a defect in telomere elongation leads to senescence in yeast. Cell *57*, 633–643.

Lydeard, J.R., Lipkin-Moore, Z., Jain, S., Eapen, V.V., and Haber, J.E. (2010). Sgs1 and exo1 redundantly inhibit break-induced replication and de novo telomere addition at broken chromosome ends. PLoS Genet. *6*, e1000973.

Nagai, S., Davoodi, N., and Gasser, S.M. (2011). Nuclear organization in genome stability: SUMO connections. Cell Res. *21*, 474–485.

Nagai, S., Dubrana, K., Tsai-Pflugfelder, M., Davidson, M.B., Roberts, T.M., Brown, G.W., Varela, E., Hediger, F., Gasser, S.M., and Krogan, N.J. (2008). Functional targeting of DNA damage to a nuclear pore-associated SUMO-dependent ubiquitin ligase. Science *322*, 597–602.

Nie, M., Aslanian, A., Prudden, J., Heideker, J., Vashisht, A.A., Wohlschlegel, J.A., Yates, J.R., and Boddy, M.N. (2012). Dual recruitment of Cdc48 (p97)-Ufd1-Npl4 ubiquitin-selective segregase by small ubiquitin-like modifier protein (SUMO) and ubiquitin in SUMO-targeted ubiquitin ligase-mediated genome stability functions. J. Biol. Chem. *287*, 29610–29619.

Niu, H., and Klein, H.L. (2017). Multifunctional roles of Saccharomyces cerevisiae Srs2 protein in replication, recombination and repair. FEMS Yeast Res. *17*, fow111.

Oum, J.-H., Seong, C., Kwon, Y., Ji, J.-H., Sid, A., Ramakrishnan, S., Ira, G., Malkova, A., Sung, P., Lee, S.E., et al. (2011). RSC facilitates Rad59-dependent homologous recombination between sister chromatids by promoting cohesin loading at DNA double-strand breaks. Mol. Cell. Biol. *31*, 3924–3937.

Oza, P., Jaspersen, S.L., Miele, A., Dekker, J., and Peterson, C.L. (2009). Mechanisms that regulate localization of a DNA double-strand break to the nuclear periphery. Genes Dev. *23*, 912–927.

Psakhye, I., and Jentsch, S. (2012). Protein group modification and synergy in the SUMO pathway as exemplified in DNA repair. Cell *151*, 807–820.

Sacher, M., Pfander, B., Hoege, C., and Jentsch, S. (2006). Control of Rad52 recombination activity by double-strand break-induced SUMO modification. Nat. Cell Biol. *8*, 1284–1290.

Schober, H., Ferreira, H., Kalck, V., Gehlen, L.R., and Gasser, S.M. (2009). Yeast telomerase and the SUN domain protein Mps3 anchor telomeres and repress subtelomeric recombination. Genes Dev. *23*, 928–938.

Silva, S., Altmannova, V., Eckert-Boulet, N., Kolesar, P., Gallina, I., Hang, L., Chung, I., Arneric, M., Zhao, X., Buron, L.D., et al. (2016). SUMOylation of Rad52-Rad59 synergistically change the outcome of mitotic recombination. DNA Repair (Amst) *42*, 11–25.

Simon, M.-N., Churikov, D., and Géli, V. (2016). Replication stress as a source of telomere recombination during replicative senescence in *Saccharomyces cerevisiae*. FEMS Yeast Res. *16*, fow085.

Smith, J., and Rothstein, R. (1995). A mutation in the gene encoding the Saccharomyces cerevisiae single-stranded DNA-binding protein Rfa1 stimulates a RAD52-independent pathway for direct-repeat recombination. Mol. Cell. Biol. *15*, 1632–1641.

Smith, J., and Rothstein, R. (1999). An allele of RFA1 suppresses RAD52-dependent double-strand break repair in Saccharomyces cerevisiae. Genetics *151*, 447–458.

Su, X.A., Dion, V., Gasser, S.M., and Freudenreich, C.H. (2015). Regulation of recombination at yeast nuclear pores controls repair and triplet repeat stability. Genes Dev *29*, 1006–1017.

Taddei, A., Hediger, F., Neumann, F.R., Bauer, C., and Gasser, S.M. (2004). Separation of silencing from perinuclear anchoring functions in yeast Ku80, Sir4 and Esc1 proteins. EMBO J. *23*, 1301–1312.

Taddei, A., Schober, H., and Gasser, S.M. (2010). The budding yeast nucleus. Cold Spring Harb. Perspect. Biol. *2*, a000612.

Teng, S.C., and Zakian, V.A. (1999). Telomere-telomere recombination is an efficient bypass pathway for telomere maintenance in Saccharomyces cerevisiae. Mol. Cell. Biol. *19*, 8083–8093.

Teng, S.C., Chang, J., McCowan, B., and Zakian, V.A. (2000). Telomerase-independent lengthening of yeast telomeres occurs by an abrupt Rad50p-dependent, Rif-inhibited recombinational process. Mol. Cell *6*, 947–952.

Whalen, J.M., and Freudenreich, C.H. (2020). Location, location, location: the role of nuclear positioning in the repair of collapsed forks and protection of genome stability. Genes (Basel) *11*, 635.

Titus, L.C., Dawson, T.R., Rexer, D.J., Ryan, K.J., and Wente, S.R. (2010). Members of the RSC chromatin-remodeling complex are required for maintaining proper nuclear envelope structure and pore complex localization. Mol Biol Cell *21*, 1072–1087.

Whalen, J.M., Dhingra, N., Wei, L., Zhao, X., and Freudenreich, C.H. (2020). Relocation of collapsed forks to the nuclear pore complex depends on sumoylation of DNA repair proteins and permits Rad51 association. Cell Rep. *31*, 107635.

Wu, Y., Siino, J.S., Sugiyama, T., and Kowalczykowski, S.C. (2006). The DNA binding preference of RAD52 and RAD59 proteins: implications for RAD52 and RAD59 protein function in homologous recombination. J. Biol. Chem. *281*, 40001–40009.

Xie, Z., Jay, K.A., Smith, D.L., Zhang, Y., Liu, Z., Zheng, J., Tian, R., Li, H., and Blackburn, E.H. (2015). Early telomerase inactivation accelerates aging independently of telomere length. Cell *160*, 928–939.

Xu, Z., Fallet, E., Paoletti, C., Fehrmann, S., Charvin, G., and Teixeira, M.T. (2015). Two routes to senescence revealed by real-time analysis of telomerase-negative single lineages. Nat. Commun. *6*, 7680.

iScience, Volume *24*

Supplemental information

Rad52 SUMOylation functions as a molecular switch that determines a balance between the Rad51- and Rad59-dependent survivors

Ferose Charifi, Dmitri Churikov, Nadine Eckert-Boulet, Christopher Minguet, Frédéric Jourquin, Julien Hardy, Michael Lisby, Marie-Noëlle Simon, and Vincent Géli

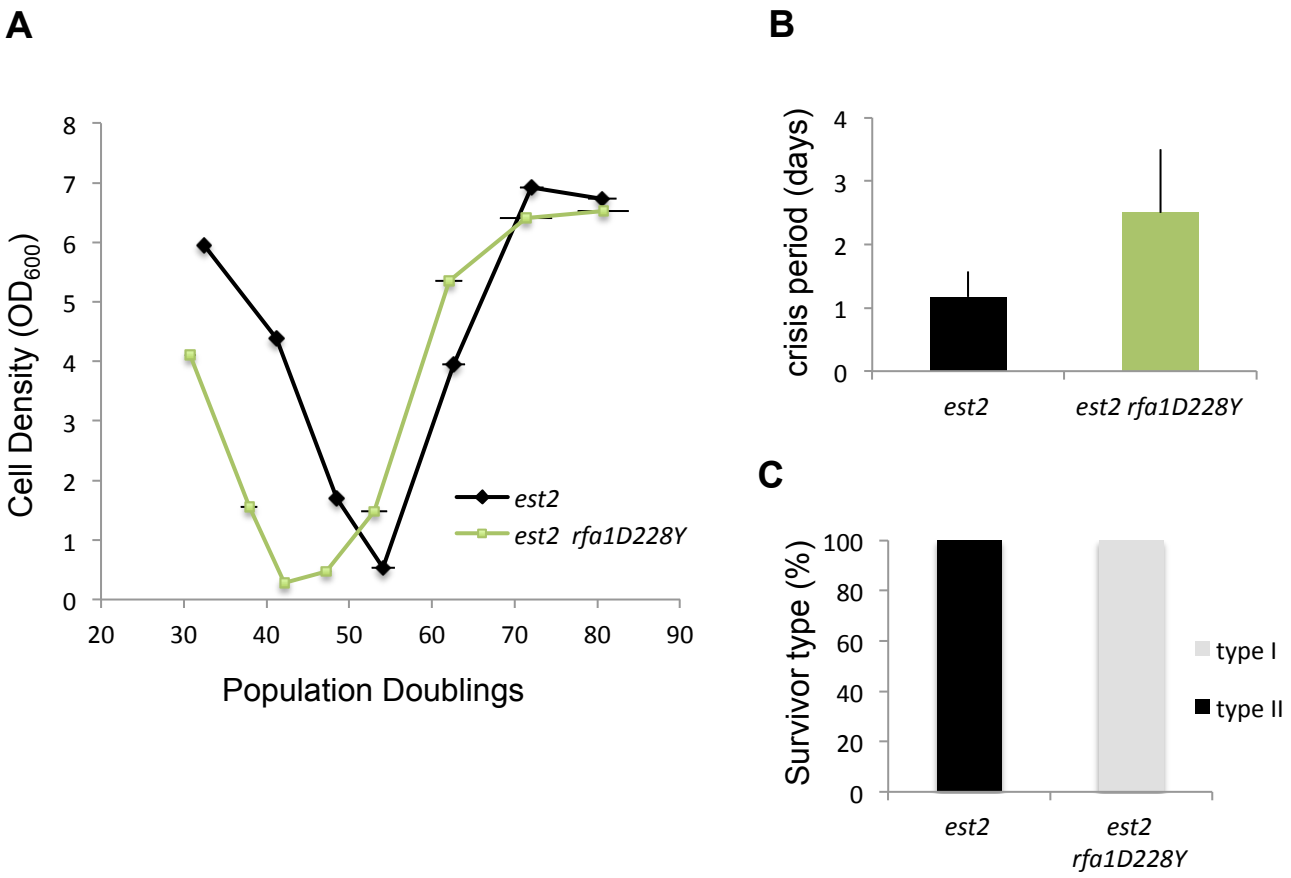

Figure S1. *rfa1-DD228Y* impairs type II recombination (related to Figure 1). (**A**) Mean senescence profiles of *est2Δ* (n=6) and *est2Δ rfa1D228Y* (n=4) clones. Bars are SD. (**B**) The crisis period is determined as the number of days the cell population stays arrested for each individual clones analyzed. Crisis period average calculated for each mutant is represented. Bars are SD (**C**). Relative frequencies of the telomerase-independent survivor types formed by the clones analyzed in (A).

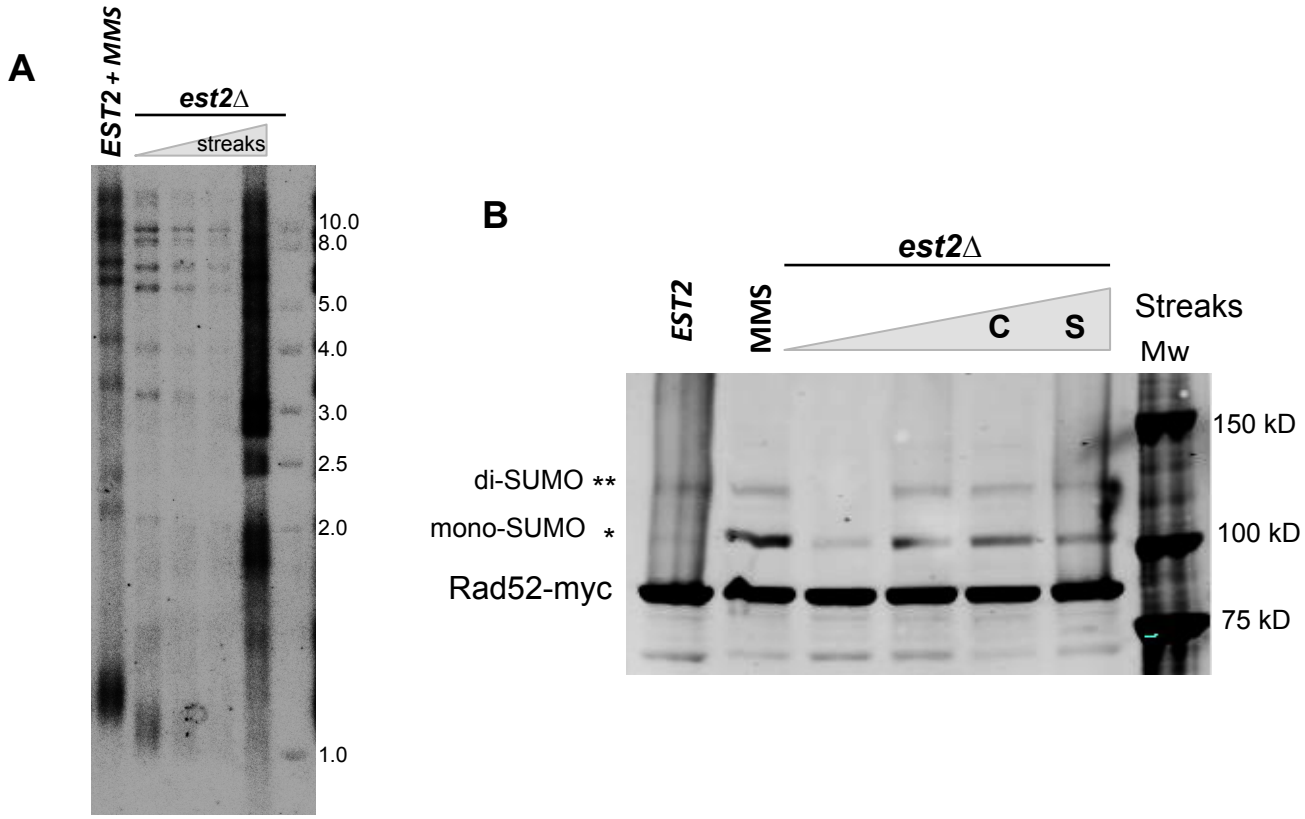

Figure S2. Rad52 is SUMOylated upon telomere erosion (Related to Figure 2). An *est2Δ RAD52-MYC* haploid strain was obtained by sporulating a heterozygous *EST2*/*est2Δ RAD52*/*RAD52-MYC* diploid strain. The *est2Δ RAD52-MYC* haploid was serially streaked 4 times on YPD plates. After each restreak, cells were collected for DNA extraction and whole cell protein extracts. (A) Telomere length was analyzed after *XhoI* DNA digestion by southern blot using a TG_{1-3} probe. (B) At each restreak, cell protein extracts were analyzed by Western-blot using an anti-MYC antibody (9E10). SUMOylated forms of Rad52 are indicated. Extracts from *EST2* cells treated or not with MMS are shown as controls. Crisis (C), Survivors (S).

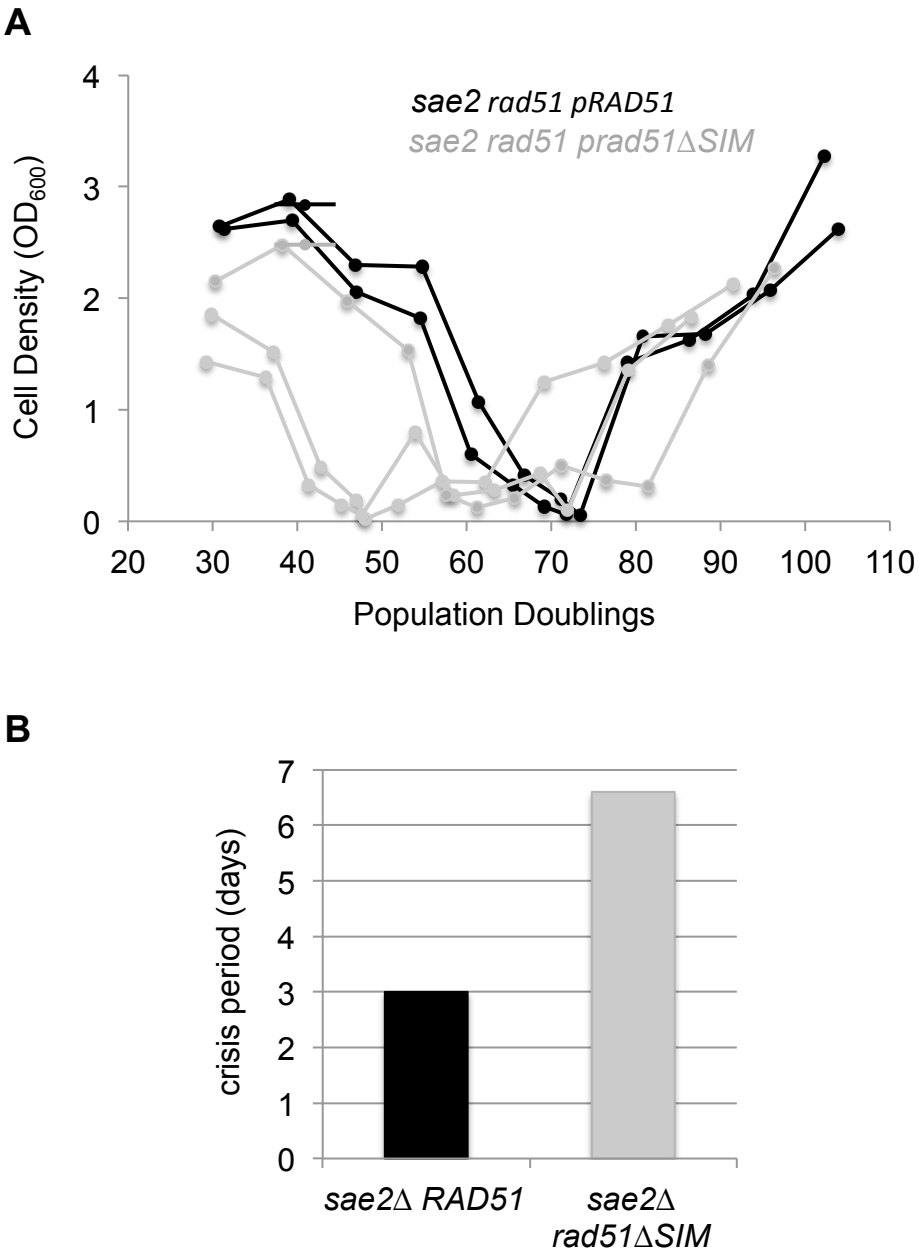

Figure S3. Deleting the SIM domains of Rad51 affects type I recombination (Related to Figure 3). **(A)** Replicative senescence profiles of *est2Δ rad51Δ sae2Δ* cells expressing either WT *RAD51* or *rad51ΔSIM* from a centromeric vector. Senescence was monitored as described above except that the liquid cultures were performed in SC-LEU to maintain the vector. Deleting the SIM domains of Rad51 delays the appearance of survivors**. (B)** Mean time spent in crisis for the clones in (A).

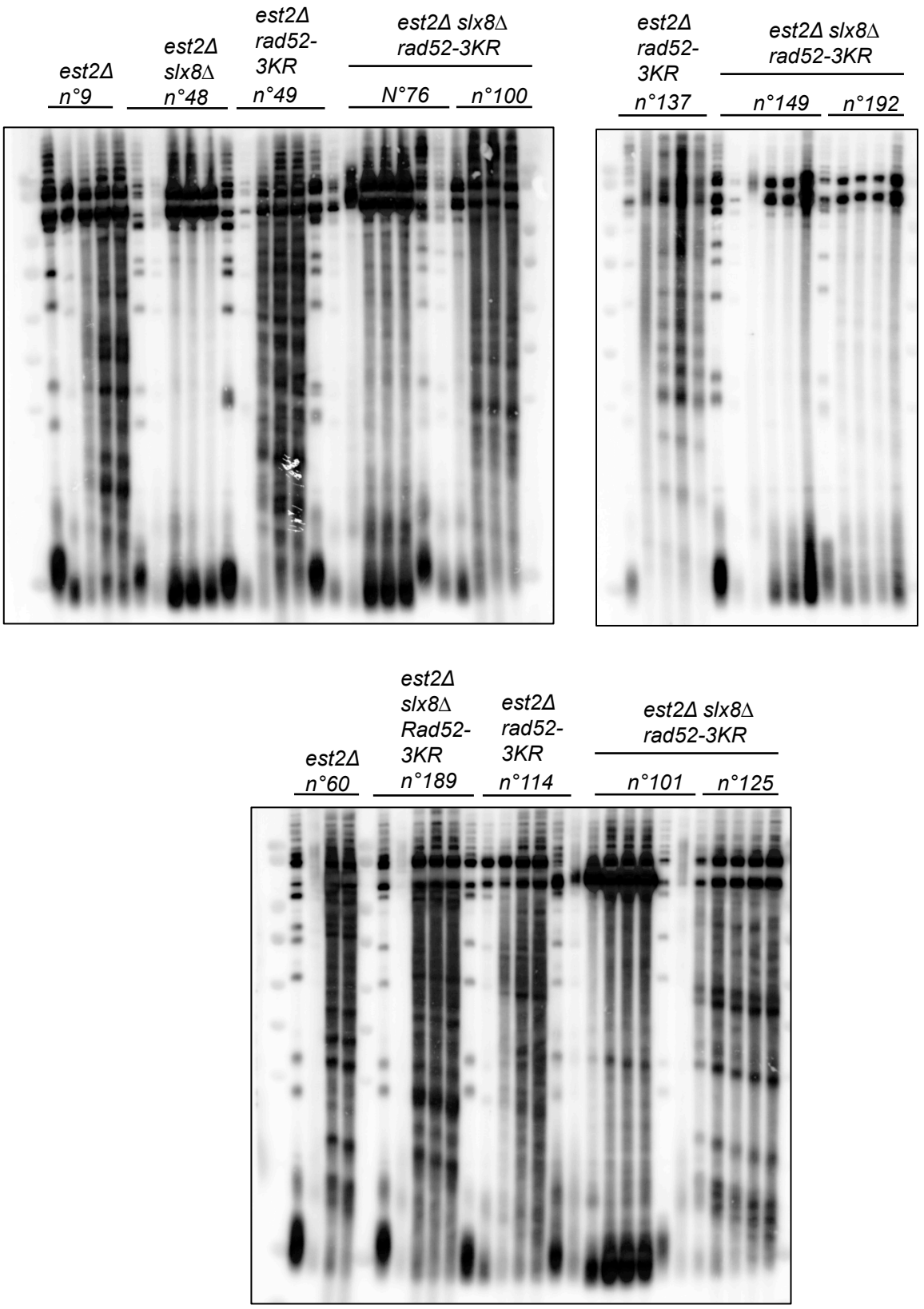

Figure S4. Representative teloblots (related to Figure 4).

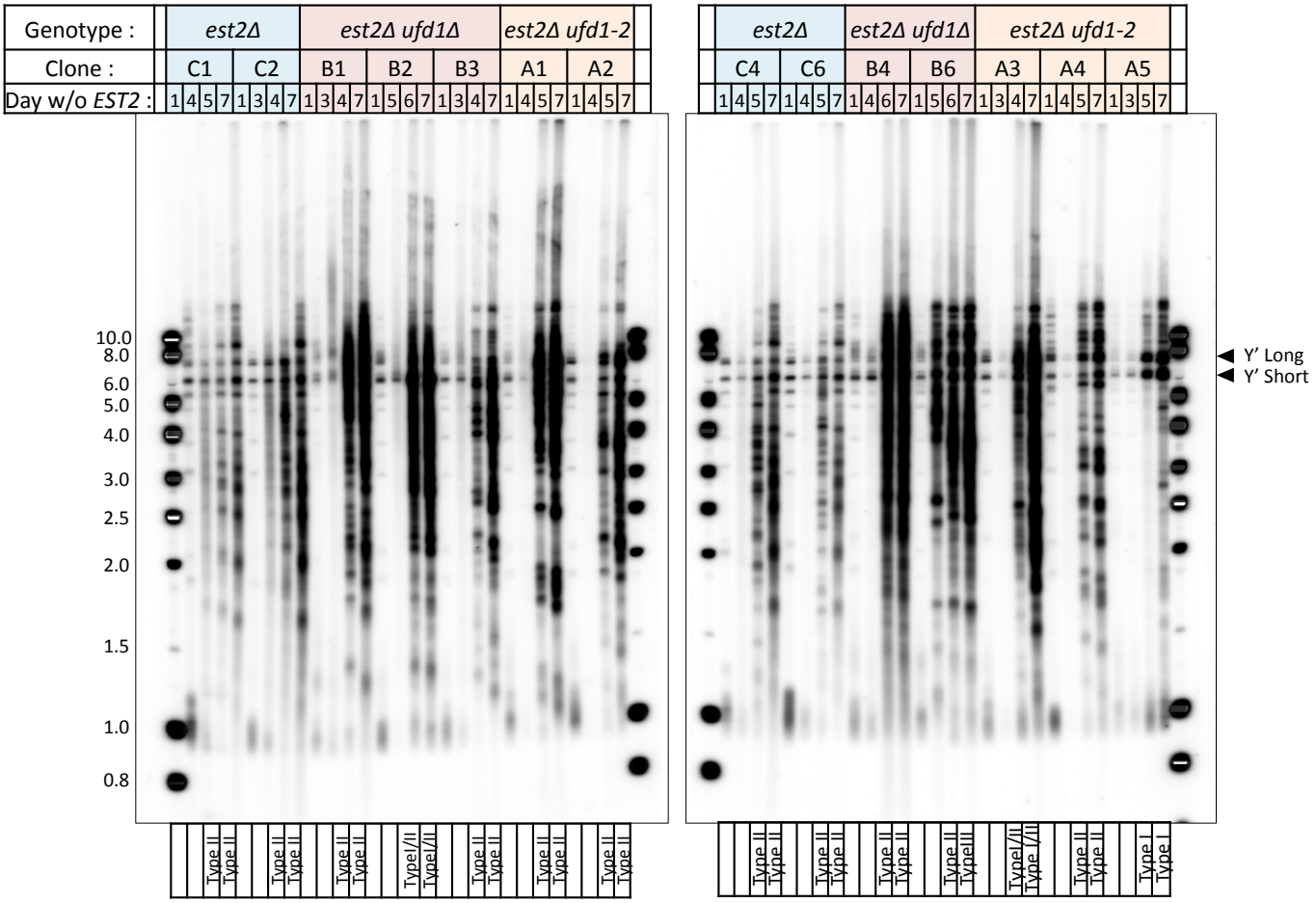

Figure S5. Representative teloblots (related to Figure 5).

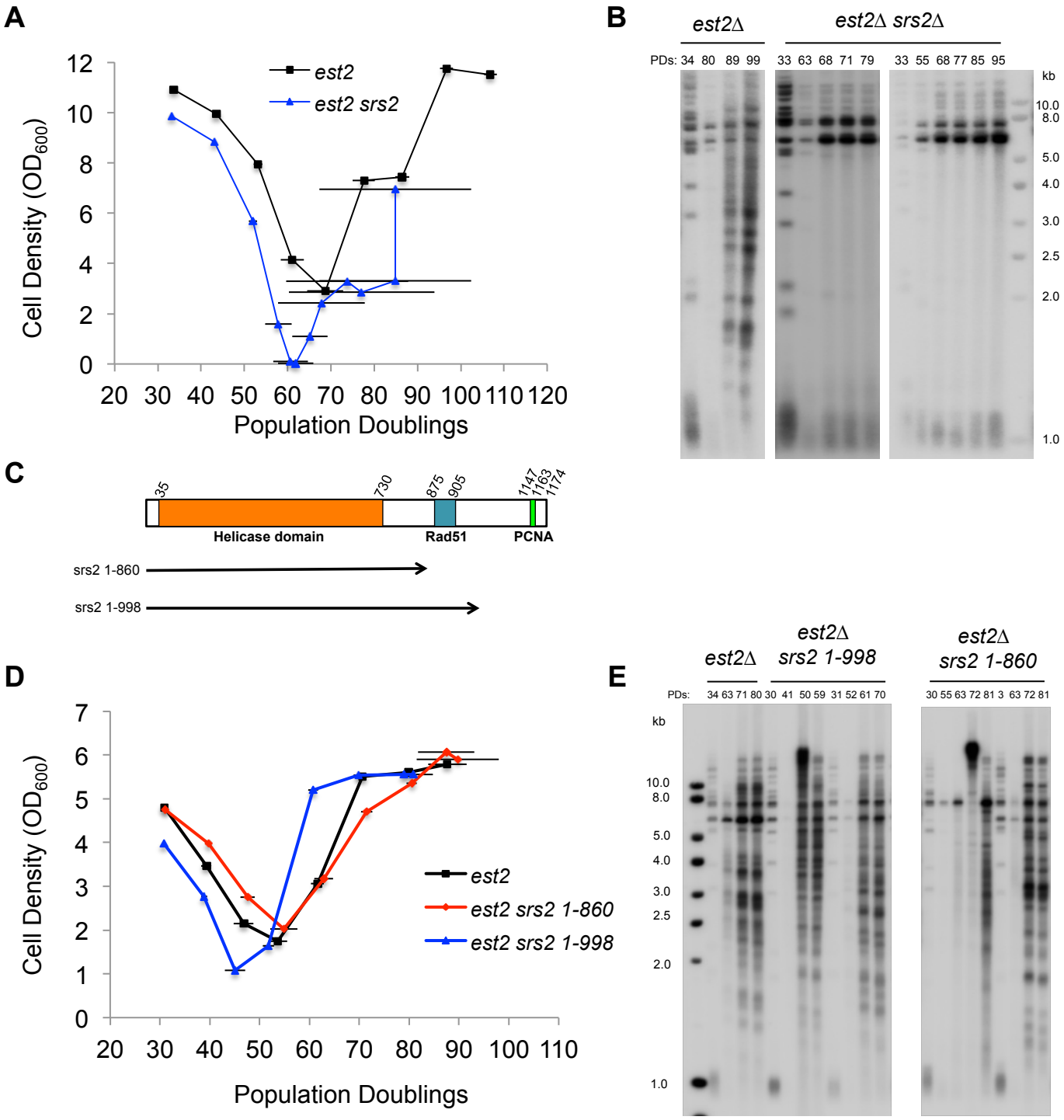

Figure S6. The helicase/antirecombinase Srs2 is required for type II recombination (Related to Figures 3 and 5). (A) Mean senescence profiles of *est2Δ* (n=5), *est2Δ srs2Δ* (n=5) clones. Bars represent SD. (**B**) Telomere length and recombination were analyzed by TG_{1-3} probed Southern blot of *XhoI*-digested DNA prepared from samples of the replicative senescence. The result for two representative clones is shown (5 clones analyzed). (**C**) Schematic representation of the domain organization of Srs2 and of the mutants used in this study. Only the helicase domain and the domains of interaction with Rad51 and PCNA are shown. (**D**) Mean senescence profiles of *est2Δ* (n=8), *est2Δ srs2 1-860* (n=4) and *est2Δ srs2 1-998* (n=10) clones. Bars represent SD. (E) Southern blot of *XhoI*-digested DNA prepared from samples of the replicative senescence. The result for two representative clones is shown for each genotypes.

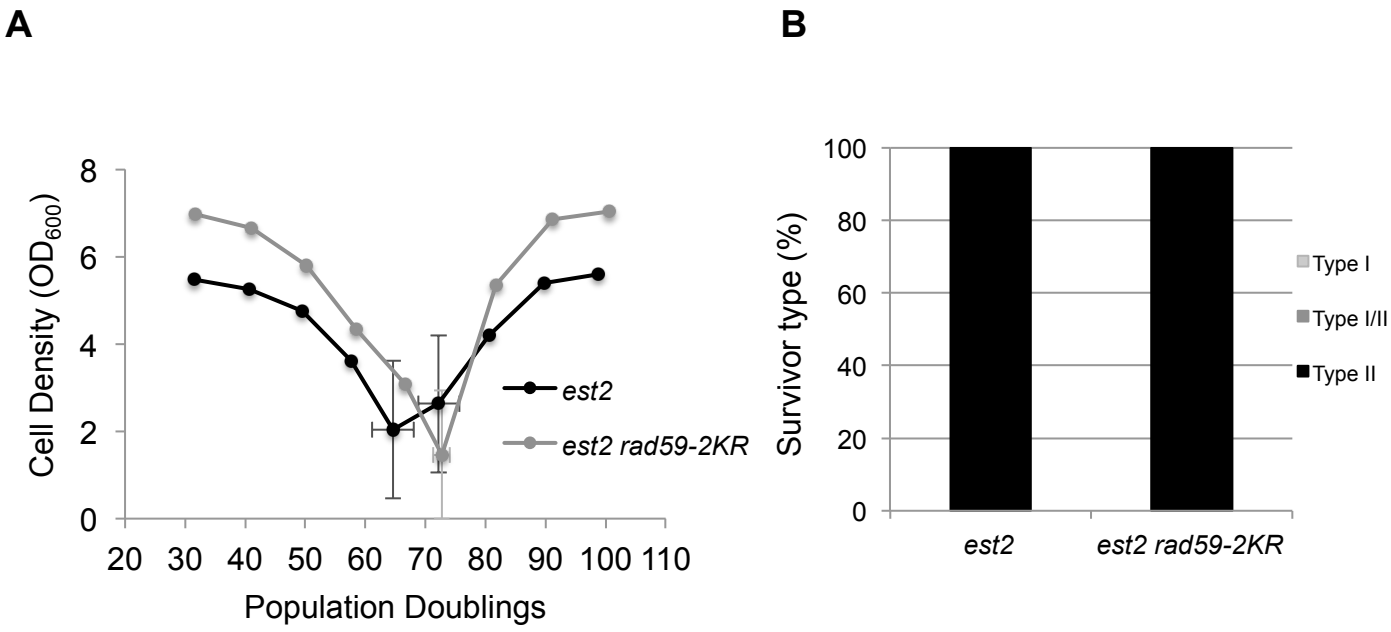

Figure S7. Abolishing Rad59 SUMOylation does not affect NPC type II recombination (Related to Figure 6).

(**A**) Replicative senescence of *est2Δ* and *est2Δ rad59-2KR (n=7)*. (**B**) Relative frequencies of the telomerase-independent survivor types for the *est2Δ* and *est2Δ rad59-2KR*.

Supplementary Table 1: Strains used in this study (related to figures 1 to 7).

Strain	Genotype[1]	Source
ML741-6A	*MAT***a** *RAD52-RFP CDC13-YFP nup133::HIS3 est2::KanMX6 rad51*Δ pNEB21 pUN100-protA-NUP133::LEU2	This study
NEB364-74B	*MAT***a** *RAD52-RFP CDC13-YFP nup133::HIS3 est2::KanMX6 rad59::KanMX6* pNEB21 pUN100-protA-NUP133::LEU2	This study
NEB162-37B	*MAT***a** *RAD52-RFP CDC13-YFP nup133::HIS3 est2::KanMX6* pNEB21 pUN100-protA-NUP133::LEU2	Khadaroo et al., 2009
TG01-8D	*MAT***a** *est2::LEU2 pEST2(URA3)*	AM Bailis
NEB153-10B	*MAT***a** *est2::kanMX6 pEST2(URA3)*	Hardy et al., 2014
DCY5H2	*MAT***a** *RAD5 rfa1-K133,170,427R rfa2-K199R rfa3-K46R* p3x*HA-SLX5* (*LEU2*) 2μ	This study
MNY1508	*MAT***a***/a EST2/est2 ::LEU2 SLX8/slx8 ::KanMX6 RFA1/ rfa1-K133,170,427R RFA2/rfa2-K199R RFA3/ rfa3-K46R*	This study
NEB142-7C	*MAT***a** *RAD5 rad52-K43,44,253R*	This study
FCY337	*MAT***a***/α EST2/est2 ::LEU2 RAD52/rad52-K*43,44,253R	This study
MNY896	*MATα sae2::TRP1*	Hardy et al., 2014
MNY896 x FCY278	*MAT***a***/α EST2/est2::LEU2 RAD52/rad52- K*43,44,253R *SAE2/sae2::TRP pEST2::URA3*	This study
MNY1016	*rad51::LEU2*	Hardy et al., 2014
MNY1016 x FCY278	*MAT***a***/α EST2/est2 ::LEU2 RAD51/rad51 ::LEU2 RAD52/rad52- K*43,44,253R	This study
ML894-4c	*MAT***a** *rfa1-K133,170,427R rfa2-K199R rfa3-K46R*	This study
DCY-5I1	*MAT***α** *rad52-myc* (*NAT*)	This study
ML236-9B	*MATα rad59::KanMX6*	This study
ML236-9B x FCY278	*MAT***a***/α EST2/est2::LEU2 RAD59/rad59::KanMX6 RAD52/rad52- K*43,44,253R	This study
FJY1	*MAT***a***/α EST2/est2 ::KanMX6 SAE2/sae2 ::TRP1 RAD51/rad51 ::KanMX6 pRAD51(LEU2)*	This study
FJY2	*MAT***a***/α EST2/est2 ::KanMX6 SAE2/sae2 ::TRP1 RAD51/rad51::KanMX6 pRAD51*Δ*SIM(LEU)*	This study
ML912-14A	*MAT***a** *RAD52-RFP CDC13-YFP nup133::HIS3 rfa1-K133,170,427R rfa2-K199R rfa3-K46R est2::KanMX6* pNEB21 pUN100-*protA-NUP133* (*LEU2*)	This study
ML825-1D	*MAT***a** *RAD52-RFP CDC13-YFP nup133::HIS3 est2::KanMX6 rad59-K207,228R* pNEB21 pUN100-*protA-NUP133* (*LEU2*)	This study
	*MAT***a***/a EST2/est2::LEU2 UFD1/ufd1*Δ*C::HPH*	This study

MNY1640	*MAT***a**/*a EST2/est2::LEU2 UFD1/ufd1-2*	This study
MNY1455	*MAT***a**/*a EST2/est2::LEU2 SLX8/slx8::KanMX6 RAD52/rad52- K*43,44,253R	This study
2070-5	*MAT***a**/*α EST2/est2 ::KanMX6 rad59::KanMX6/ rad59-K207,228R*	This study
MNY1460	*MAT***a**/*α EST2/est2::KanMX6 NUP1/nup1-LexA::TRP1 SRS2/ srs2::HIS pEST2::URA3*	This study
2070-5	*srs2 2-860::HPH*	Hannah Klein
MNY1522	*MAT***a**/*α EST2/est2::KanMX6 NUP1/nup1-LexA::TRP SRS2/ srs2 2-860::HPH*	This study
MNY1527	*MAT***a**/*α EST2/est2::LEU2 NUP1/nup1-LexA::TRP1 SRS2/srs2 1-998::KanMX6*	This study
MNY1597	*MAT***a**/*α EST2/est2::KanMX6 NUP1/nup1-LexA::TRP1 RFA1/rfa1-D228Y pEST2::URA3*	This study
MNY1528	*Type II survivors MAT***a**/*α est2::LEU2/est2::LEU2 SRS2/srs2::HIS3*	This study
MNY1542	*Type II survivors MAT***a**/*α est2::LEU2/est2::LEU2 PIF1/pif1::KanMX6*	This study
MNY1548	*Type II survivors MAT***a**/*α est2::LEU2/ est2::LEU2 SLX8/slx8::KanMX6*	This study
MNY1565	*Type II survivors MAT***a**/*α est2::LEU2/ est2::LEU2 RAD51/rad51::KanMX6*	This study
MNY1563	*Type II survivors MAT***a**/*α est2::LEU2/ est2::LEU2 RAD59/rad59::KanMX6*	This study

[1] Yeast strains in this study are derivatives of W303-1A (*MAT***a** *BAR1 LYS2 ade2-1 can1-100 ura3-1 his3-11,15 leu2-3, 112 trp1-1 rad5-535*) (Thomas and Rothstein, 1989).

TRANSPARENT METHODS

Strains and Senescence assays

Strains used in this study are described in Table S1. Liquid senescence assays were performed starting with the haploid spore products of diploids that were heterozygous for EST2 (*EST2*/*est2Δ*) and for the gene(s) of interest. To ensure homogeneous telomere length before sporulation, the diploids were propagated for at least 50 PDs in YPD. The entire colonies outgrowing from haploid spores (estimated 20-30 PDs) were inoculated in liquid YPD medium to estimate the number of PDs, diluted to OD600= 0,1 and grown at 30°C. Every 24 hrs, the cell density was measured (OD_{600}), and a fresh 15 ml of YPD culture was inoculated at an estimated density of 10^5 cells per ml. Multiple clones of each genotype were propagated in this manner until the emergence of survivors. Replicative senescence curves shown in this study correspond to the average of several senescence using independent spores with identical genotype. When indicated, the number of days the cell population stays arrested (crisis period) was determined for each individual spore. Senescence assays on solid medium were initiated as described above, but the cells were propagated by consecutive restreaking on solid YPD plates followed by outgrowth for 2 days at 30°C. The process was repeated until the appearance of survivors. Telomere lengths were analyzed by Southern blotting of *XhoI* cut genomic DNA probed with a telomeric TG_{1-3} probe. Type I and II survivors were determined based on their characteristic terminal restriction fragment pattern (Simon et al., 2021). When both type I and II survivors were detected in the same culture, the type was scored as mixed.

Coimmunoprecipitation

Native protein extracts were prepared in HNT buffer (50 mM HEPES, 200 mM NaCl, 1% Triton X-100) at pH 7.5 by cell disruption with glass beads in a Precellys 24 homogenizer (BertinTechnologies, France). To minimize protein degradation and loss of PTMs, the buffer was supplemented with protease inhibitors: 30 mM N-ethylmaleimide (NEM), 1 mM sodium orthovanadate, and EDTA-free complete cocktail (Roche). For IPs the extracts were rotated top over bottom, first for 2 hr with either anti-HA (3F10) or anti-yRFA antibodies, and then for another 1.5 hr with Dynabeads protein G (Invitrogen Dynal AS, Oslo, Norway) at 4°C. The beads were then subjected to stringent washing (5 times in HNT buffer) to remove non-specific background binding to the beads. The bound proteins were eluted by boiling the beads in the Laemmli sample buffer and subjected to immunoblotting. For the experiment

shown in Fig. 1, the extracts were treated with 100 mg/mL of DNase I (Roche) for 30 min on ice prior to IP.

Live cell imaging of senescing cells and fluorescence microscopy

Live-cell imaging was performed on *est2Δ nup133ΔN* cells expressing Rad52-RFP, Cdc13-YFP and CFP-Nup49 (pNEB21) tagged proteins after loss of the pVL291 vector carrying *EST2* (*URA3*) by restreaking on SC-Trp plates and testing for the loss of pEST2-URA3 by replica-plating onto SC-Ura, (Churikov et al., 2016; Khadaroo et al., 2009). Two-to-four independent Ura^- and $5\text{-}FOA^R$ colonies were used to inoculate 20-ml liquid cultures in SC-Trp-Leu+Ade medium (100 μg/ml adenine). These cultures were grown in the shaker incubator at 25°C and diluted to OD_{600} = 0.3 every day. At the time of each dilution, an aliquot of cells was examined by fluorescence microscopy. Generation time was calculated based on OD_{600} measured over consecutive time intervals. Mutant strains (*rad51Δ, rad59Δ*, *rad59-2KR*) were obtained by sporulation of respective hetorozygous diploids followed by selection of spore clones carrying desired combination of markers. Fluorescence microscopy was performed as described (Eckert-Boulet et al., 2011).

Western Blot and antibodies

Protein extracts for Western blot analysis were prepared from trichloroacetic acid (TCA)-treated yeast cells (Azzam et al., 2004). Proteins were resolved on 10% SDS-PAGE and analyzed by standard Western blotting techniques. Monoclonal antibody against the MYC-epitope (9E10) was used to detect Rad52-Myc. Rabbit polyclonal serum against *S. cerevisiae* RFA (AS07 214) was obtained from Agrisera.

Supplemental references:

Azzam, R., Chen, S.L., Shou, W., Mah, A.S., Alexandru, G., Nasmyth, K., Annan, R.S., Carr, S.A., and Deshaies, R.J. (2004). Phosphorylation by cyclin B-Cdk underlies release of mitotic exit activator Cdc14 from the nucleolus. Science *305*, 516–519.

Churikov, D., Charifi, F., Eckert-Boulet, N., Silva, S., Simon, M.-N., Lisby, M., and Géli, V. (2016). SUMO-Dependent Relocalization of Eroded Telomeres to Nuclear Pore Complexes Controls Telomere Recombination. Cell Rep *15*, 1242–1253.

Eckert-Boulet, N., Rothstein, R., and Lisby, M. (2011). Cell biology of homologous recombination in yeast. Methods Mol Biol *745*, 523–536.

Hardy, J., Churikov, D., Géli, V., and Simon, M.-N. (2014). Sgs1 and Sae2 promote telomere replication by limiting accumulation of ssDNA. Nat Commun *5*, 5004.

Khadaroo, B., Teixeira, M.T., Luciano, P., Eckert-Boulet, N., Germann, S.M., Simon, M.N., Gallina, I., Abdallah, P., Gilson, E., Géli, V., et al. (2009). The DNA damage response at eroded telomeres and tethering to the nuclear pore complex. Nat Cell Biol *11*, 980–987.

Simon, M.N., Churikov, D. and Geli, V. (2021) Analysis of recombination at yeast telomeres. Methods Mol Biol *2153*, 395-402.

Thomas, B.J. and Rothstein, R. (1989) The genetic control of direct-repeat recombination in *Saccharomyces*: the effect of rad52 and rad1 on mitotic recombination at GAL10, a transcriptionally regulated gene . Genetics *123*, 725-738.